

BOLU ABANT IZZET BAYSAL UNIVERSITY
THE GRADUATE SCHOOL OF NATURAL AND APPLIED
SCIENCES
DEPARTMENT OF CHEMISTRY



EFFECT OF SYMMETRIC AND ASYMMETRIC HEAD
GROUP GROWTH OF IONIC SURFACE ACTIVE
MOLECULE ON LYOTROPIC UNIAXIAL-TO-BIAXIAL
NEMATIC PHASE TRANSITIONS

MASTER OF SCIENCE

EMRE GÜNER

BOLU, JANUARY 2019

APPROVAL OF THE THESIS

EFFECT OF SYMMETRIC AND ASYMMETRIC HEAD GROUP GROWTH OF IONIC SURFACE ACTIVE MOLECULE ON LYOTROPIC UNIAXIAL-TO-BIAXIAL NEMATIC PHASE TRANSITIONS submitted by EMRE GUNER in partial fulfillment of the requirements for the degree of Master of Science in Department of Chemistry, The Graduate School of Natural and Applied Sciences of BOLU ABANT IZZET BAYSAL UNIVERSITY in 18/01/2019 by

Examining Committee Members

Signature

Supervisor
Assoc. Prof. Dr. Erol AKPINAR
Abant Izzet Baysal University



Member
Assoc. Prof. Dr. Öznur DEMİR ORDU
Abant Izzet Baysal University



Member
Assoc. Prof. Dr. Abdulkadir ALLI
Duzce University



Graduation Date :

Prof. Dr. Ömer ÖZYURT



Director of Graduate School of Natural and Applied Sciences

To my family



DECLARATION

I hereby declare that all information in this document has been obtained and presented in accordance with academic rules and ethical conduct. I also declare that, as required by these rules and conduct, I have fully cited and referenced all material and results that are not original to this work.

EMRE GÜNER

A handwritten signature in blue ink, appearing to read 'Emre Güner', is positioned below the printed name.

ABSTRACT

EFFECT OF SYMMETRIC AND ASYMMETRIC HEAD GROUP GROWTH OF IONIC SURFACE ACTIVE MOLECULE ON LYOTROPIC UNIAXIAL-TO-BIAXIAL NEMATIC PHASE TRANSITIONS

MSC THESIS

EMRE GÜNER

BOLU ABANT IZZET BAYSAL UNIVERSITY GRADUATE SCHOOL OF
NATURAL AND APPLIED SCIENCES

DEPARTMENT OF CHEMISTRY

(SUPERVISOR: ASSOC. PROF. DR. EROL AKPINAR)

BOLU, JANUARY 2019

Lyotropic quaternary mixtures of some tetradecylalkylammonium bromides (tetradecyldimethylammonium bromide, TDMABr; tetradecyltrimethylammonium bromide, TTMABr; tetradecyldimethylethylammonium bromide, TDMEABr; tetradecyldiethylmethylammonium bromide, TDEMABr; tetradecyltriethylammonium bromide, TTEABr; tetradecyltripropylammonium bromide, TTPABr; tetradecyltributylammonium bromide, TTBABr), were prepared to examine the effect of the symmetric and asymmetric head-group growth of the surfactants on the stabilization of different lyotropic nematic phases and uniaxial-to-biaxial phase transitions. The lyotropic mixtures were prepared by the dissolution of the tetradecylalkylammonium bromides (TAABr) in the mixture of NaBr/DeOH/water. The textures of the lyotropic mesophases were characterized by polarizing optical microscope. The uniaxial-to-biaxial nematic phase transitions were determined from the temperature dependence of the birefringences of the nematic phases via laser conoscopy. The results indicated that the head-group size of the surfactant molecules influences both the amphiphilic molecular aggregate topology and uniaxial-to-biaxial nematic phase transitions, and, in addition, the minimum area per surfactant head group is a key parameter on stabilizing the lyotropic biaxial nematic phase.

KEYWORDS: Lyotropic nematic phases, uniaxial-to-biaxial nematic phase transition, laser conoscopy, birefringences, minimum area per surfactant head group, degree of counterion binding, conductivity.

ÖZET

İYONİK YÜZEY AKTİF MOLEKÜLLERİN BAŞ GRUPLARINDAKİ SİMETRİK VE ASİMETRİK BÜYÜMENİN LİYOTROPİK TEK EKSENLİ-ÇİFT EKSENLİ NEMATİK FAZ GEÇİŞLERİ ÜZERİNE ETKİSİ

YÜKSEK LİSANS TEZİ

EMRE GÜNER

BOLU ABANT İZZET BAYSAL ÜNİVERSİTESİ

FEN BİLİMLERİ ENSTİTÜSÜ

KİMYA ANABİLİM DALI

(TEZ DANIŞMANI: DOÇ. DR. EROL AKPINAR)

BOLU, OCAK - 2019

Bazı tetradetilalkilamonyum bromürlerin (tetradesildimetilamonyum bromür, TDMABr; tetradesiltrimetilamonyum bromür, TTMABr; tetradesildimetiletilamonyum bromür, TDMEABr; tetradesildietilmetilamonyum bromür, TDEMABr; tetradesiltriethylamonyum bromür, TTEABr; tetradesiltripropilamonyum bromür, TTPABr; tetradesiltribütülamonyum bromür, TTBABr) liyotropik dört bileşenli karışımları, sürfaktant baş gruplarının simetrik ve asimetric büyümesinin farklı liyotropik nematik fazların stabilizasyonu ve tek eksenli-çift eksenli faz geçişleri üzerine etkisini incelemek için hazırlanmıştır. Liyotropik karışımlar, tetradetilalkilamonyum bromürlerin (TAABr) NaBr/DeOH/su çözeltisi içerisinde çözünmesiyle hazırlanmıştır. Liyotropik mezofazların dokuları polarize optik mikroskopu ile karakterize edilmiştir. Tek eksenli-çift eksenli nematik faz geçişleri lazer konoskopi ile nematik fazların çift kırınımalarının sıcaklığa bağımlılığında belirlenmiştir. Sonuçlar, sürfaktantların baş grubu boyutunun amfifilik moleküler kümelenme topolojisini ve tek eksenli-çift eksenli faz geçişlerini etkilediğini, ve buna ek olarak sürfaktant baş grubu başına düşen minimum alanın liyotropik çift eksenli fazın stabilizasyonunda anahtar bir parametre olduğunu göstermiştir.

ANAHTAR KELİMELER: Liyotropik nematik fazlar, tek eksenli-çift eksenli nematik faz geçişi, lazer konoskopi, çift kırınım, sürfaktant baş grubu başına düşen minimum alan, karşı-iyon bağlanma derecesi, iletkenlik.

TABLE OF CONTENTS

	<u>Page</u>
ABSTRACT	v
ÖZET	vi
TABLE OF CONTENTS	vii
LIST OF FIGURES	viii
LIST OF TABLES	xi
LIST OF ABBREVIATIONS AND SYMBOLS	xii
1. INTRODUCTION	1
1.1 Classification of Liquid Crystals	2
1.1.1 Lyotropic Liquid Crystalline Structures	3
1.1.1.1 Lyotropic Nematic LC Phases (N).....	4
1.1.1.2 Optical and Magnetic Properties of Nematic Phases	14
1.2 As a Precursor of Lyotropic Nematic Phases: Isotropic Micellar Solutions	17
1.2.1 Thermodynamic Parameters of Micellization.....	19
2. AIM AND SCOPE OF THE STUDY	21
3. MATERIALS AND METHODS	24
3.1 Chemicals	24
3.2 Electrical Conductivity	31
3.3 Preparation Process of Liquid Crystal Samples	32
3.4 Laser Conoscopy	32
3.5 Polarizing Optical Microscopy	36
4. RESULT AND DISCUSSION	37
5. CONCLUSIONS	51
6. REFERENCES	52
7. CURRICULUM VITAE	59

LIST OF FIGURES

	<u>Page</u>
Figure 1.1 Schematic representation of varying state of molecule, which forms thermotropic phases with altered temperature.	2
Figure 1.2 Molecular structure of a surfactant molecule. While the hydrophilic part is soluble in water, the hydrophobic part is not.	3
Figure 1.3 Characteristic textures for lyotropic nematic samples captured under polarizing optical microscope, where (a) N_D^- (b) N_B^- (c) N_B^+ (d) N_C^+ phases are shown. The (-) and (+) signs in the representation of the nematic phases correspond to the orientation of their optical axes with respect to the magnetic field direction (see part 1.1.1.2 for further information on the orientation of the optical axis of the nematic phases.).....	4
Figure 1.4 Orientations of (a) disc-like and (b) cylindrical-like micelles perpendicular and parallel, respectively, to magnetic field direction, H, along z. n (phase director or optical axis) represents the preferred alignment of the individual micelles with their local directors.	5
Figure 1.5 Phase diagram of KL/DeOH/water mixture which was constructed for the first time in the Ref (Yu and Saupe, 1980).....	6
Figure 1.6 (a) Partial phase diagram of SDS/DeOH/water mixture given in the Ref (Bartolino, 1982). (b) The birefringences of the uniaxial nematic phases were for the sample of 35.8% SDS.....	7
Figure 1.7 (a) Sketch of the orthorhombic micelle in the framework of the IBM model. The detergent amphiphilic bilayer is represented by C'. (b) N_D phase (c) N_B phase and (d) N_C phase.	10
Figure 1.8 Schematic representation of an ellipsoid, which is a model aggregate for the N_C phase, with the three orthogonal axes, proposed in the Ref. (Hendrikx, 1986).....	11
Figure 1.9 Schematic representation of shape of a goethite particle.....	13
Figure 1.10 A well-aligned texture of uniaxial (a) N_D (homeotropic alignment) and (b) N_C (planar alignment) phases. A: analyzer; P: polarizer; B: magnetic field direction; x, y and z are the laboratory frame axes.	15
Figure 1.11 (a) The conoscopic investigations of well-aligned textures of uniaxial nematic phases, which show characteristic cross dark brushes. An interference figure, i.e. cross dark brushes, indicates a perfect alignment of the optical axis of a nematic phase. Interference colors of nematic phases for (b) $\Delta n > 0$ and (c) $\Delta n < 0$ as a $\frac{1}{4} \lambda$ retardation plate is inserted in the light path of the polarizing light microscope. Blue arrows represent the direction of the plate....	15
Figure 1.12 Classification of surfactant types and their corresponding surfactant molecule examples.	18

Figure 1.13	Schematic representation of micelle formation via dynamic equilibrium among air/water interface adsorbed surfactant monomers, surfactant monomers in water and micelles.	18
Figure 1.14	Representation of methods used for critical micelle concentration (Nesměrák, 2006).	19
Figure 1.15	Conductivity vs concentration plot where S_1 and S_2 terms indicates the slopes before and after critical micelle concentration, respectively.....	20
Figure 3.1	Molecular structures of tetradecylalkylammonium bromides (a) tetradecyldihydrogenmethylammonium bromide, (b) tetradecyldimethylhydrogenammonium bromide, (c) tetradecyltrimethylammonium bromide, (d) tetradecyldimethylethylammonium bromide, (e) tetradecyldiethylmethylammonium bromide, (f) tetradecyltriethylammonium bromide, (g) tetradecyltripropylammonium bromide, (h) tetradecyltributylammonium bromide, (i) tetradecyltripentylammonium bromide.....	26
Figure 3.2	FT-IR spectroscopy of tetradecyldihydrogenmethylammonium bromide molecule.....	27
Figure 3.3	FT-IR spectroscopy of tetradecyldimethylhydrogenammonium bromide molecule.....	27
Figure 3.4	FT-IR spectroscopy of tetradecyltrimethylammonium bromide molecule.....	28
Figure 3.5	FT-IR spectroscopy of tetradecyldimethylethylammonium bromide molecule.....	28
Figure 3.6	FT-IR spectroscopy of tetradecyldiethylmethylammonium bromide molecule.....	29
Figure 3.7	FT-IR spectroscopy of tetradecyltriethylammonium bromide molecule.....	29
Figure 3.8	FT-IR spectroscopy of tetradecyltripropylammonium bromide molecule.....	30
Figure 3.9	FT-IR spectroscopy of tetradecyltributylammonium bromide molecule.....	30
Figure 3.10	FT-IR spectroscopy of tetradecyltripentylammonium bromide molecule.....	31
Figure 3.11	(a) Indicatrices for (a) an isotropic, (b) uniaxial positive anisotropic and (c) uniaxial negative anisotropic materials (Wahlstrom, 1969; Stoiber, 1994; Simões, 2019).....	33
Figure 3.12	(a) Biaxial positive indicatrix, (b) Biaxial negative indicatrix. OA: optical axis; CS: circular section; Bxa: Acute bisectrix; Bxo: Obtuse bisectrix (Simões, 2019.....	34
Figure 3.13	In the laser conoscopy techniques, it is assumed that micelles are thought to have orthorhombic symmetry in three nematic phases as proposed in the IBM model, given in the Figure 4a. The laboratory frame axes were defined as follows: the horizontal plane was defined by the two orthogonal axes 1 and 2; the magnetic field was aligned along the axis 1; axis 3 was vertical and parallel to the laser beam propagation direction.....	34
Figure 3.14	Representation of laser conoscopy system with details.....	35

Figure 4.1 Textures of the tetradecylalkylammonium bromide surfactants observed by polarizing optical microscopy: (a) L_{α} for TDMABr at 35.0°C, (b) N_C for TDEMABr at 15.0°C, (c) N_C+H_1 for TDEMABr at 25.0°C and (d) H_1 for TDEMABr at 55.0°C. Magnification of objective: 10x and the sample thicknesses are 200 μm	38
Figure 4.2 Temperature dependence of the birefringences, Δn (●) and δn (○), for mixtures with (a) TTMABr, (b) TDMEABr, and (c) TDEMABr. N_D , N_B and N_C are the lyotropic discotic nematic, biaxial nematic and calamitic nematic phases, respectively. H_1 is the hexagonal phase. I represent the isotropic phase.	40
Figure 4.3 Specific conductivity versus total TTMABr concentration at 30.0±0.1°C. For other TAABr surfactants, similar results were obtained. Solid lines are linear fits to the experimental points.	44
Figure 4.4 Specific conductivity versus total TDMABr concentration at 30.0±0.1°C.	44
Figure 4.5 Specific conductivity versus total TDMEABr concentration at 30.0±0.1°C.	45
Figure 4.6 Specific conductivity versus total TDEMABr concentration at 30.0±0.1°C.	45
Figure 4.7 Specific conductivity versus total TTEABr concentration at 30.0±0.1°C.	46
Figure 4.8 Specific conductivity versus total TTPrABr concentration at 30.0±0.1°C.	46
Figure 4.9 Specific conductivity versus total TTBuABr concentration at 30.0±0.1°C.	47
Figure 4.10 (a) Critical micelle concentrations, (b) degree of counterion bindings and (c) micellization Gibbs free energies of TAABr surfactants. n is the number of carbon atoms in the headgroups of the surfactants, where $n=2, 3, 4, 5, 6, 9$ and 12 correspond to TDMABr, TTMABr, TDMEABr, TDEMABr, TTEABr, TTPrABr and TTBuABr, respectively.	49

LIST OF TABLES

	<u>Page</u>
Table 4.1 Lyotropic mixture compositions in mole % and the observed phase types of the studied tetradecylalkylammonium bromides.....	37
Table 4.2 Critical micelle concentrations (cmc) of tetradecylalkylammonium bromide surfactants at 30°C. The numbers between parentheses are from literature.....	48



LIST OF ABBREVIATIONS AND SYMBOLS

LC	: Liquid crystal
LLCs	: Lyotropic liquid crystals
TLCs	: Thermotropic liquid crystals
MCD	: A mixture of disc-like and cylindrical-like micelles model.
IBM	: Intrinsically biaxial micelles model
N	: Nematic phase
N_D	: Discotic nematic phase
N_B	: Biaxial nematic phase
N_C	: Calamitic nematic phase
I	: Isotropic phase
L_α	: Lamellar phase
H₁	: Hexagonal phase
A	: Analyzer
P	: Polarizer
H	: Magnetic field
Δn/δn	: Birefringences
Δχ	: Diamagnetic susceptibility anisotropy
cmc	: Critical micelle concentration
X	: Mole fraction
κ	: Conductivity
α	: The degree of counterion ionization
β	: The degree of counterion binding to micelle
ΔG⁰_{mic}	: The standard Gibbs free energy of the micellization
ΔH⁰_{mic}	: The standard enthalpy of the micellization
ΔS⁰_{mic}	: The standard entropy of the micellization
R	: Ideal gas constant
T	: Temperature
OA	: Optical axis
CS	: Circular section
a_s	: Surface area per surfactant head group
Π	: Packing parameter

V_{hyd} : Volume of the hydrophobic chain
 l_{max} : Maximum length of the hydrophobic chain of the surfactant



ACKNOWLEDGEMENTS

The author wishes to express his deepest gratitude to his supervisor Assoc. Prof. Dr. Erol AKPINAR for his guidance, advice, criticism, encouragements and insight throughout the research.

The author would like to thank Assoc. Prof. Dr. Öznur DEMİR ORDU for her suggestions and comments.

I would also like to thank laboratory of Liquid Crystal and Soft Material Research group at BAIBU.

Finally, I must express my very profound gratitude to my parents for providing me with unfailing support and continuous encouragement throughout my years of study and through the process of researching and writing this thesis.

This study was supported by the Scientific and Technological Research Council of Turkey (TÜBİTAK), Grant No: 217Z079.

1. INTRODUCTION

In nature, there are well described three states of matter: solid, liquid and gas. Up to now, scientists could achieve to define main characteristic properties of these three main phases but the intermediate phases between those phases are still waiting for being discovered. One of these important intermediate phases is liquid crystals (LCs). First breakthrough on liquid crystals started by Austrian plant botanist Friedrich Reinitzer and German physicist Otto Lehmann in 1888 with an unexpected discovery and their heritage could shed light on the future and caused to lots of inventions in the fields of pharmacology, technology, biology and polymer industry etc. Because liquid crystals are the intermediate state of matter between isotropic liquid and anisotropic solid, while they flow like a liquid, they have orientational order and optical anisotropy like crystals.

Making a contribution to understand liquid crystals and get reveal its new aspects, one of the subclasses of liquid crystals, lyotropic liquid crystals (LLC), has been using for several years. Lyotropic liquid crystals can be formed by dissolving amphiphilic molecules (or surfactants) in a suitable solvent. Similar to isotropic micellar solutions, LLCs are obtained from the agglomeration of amphiphilic molecules by forming a supramolecular structure, so-called 'micelles'. According to the experimental studies, reported in the literature, temperature and concentration dependent LLCs have similar properties with isotropic micellar solutions. For better understanding the properties of LLCs, some information obtained from the isotropic micellar solutions exhibits a crucial importance. The aim of this thesis is to provide new findings about effect of symmetric and asymmetric head growth of surfactants on stabilizing different lyotropic liquid crystals, especially biaxial nematic phase, and uniaxial-to-biaxial phase transitions.

1.1 Classification of Liquid Crystals

Liquid crystals (LCs) are distinct states of matter located between liquid and solid states, because of this they show characteristic properties of both solids and liquids. The LCs are subdivided into two categories as: (a) thermotropic liquid crystals (TLCs) and (b) lyotropic liquid crystals (LLCs). Thermotropic liquid crystals can be generated by changing temperature for a thermotropic material and different TLC phases are formed. One can obtain this intermediate condensed phase by melting a solid material or cooling a liquid material (Figure 1.1). In 1888, Austrian botanist Reinitzer observed two melting points from the sample that he extracted from a carrot and this unforeseen discovery led to lots of technological developments (Reinitzer, 1888). Liquid crystal displays (LCDs), thermometers and lots of optical devices can be given as examples of these developments.

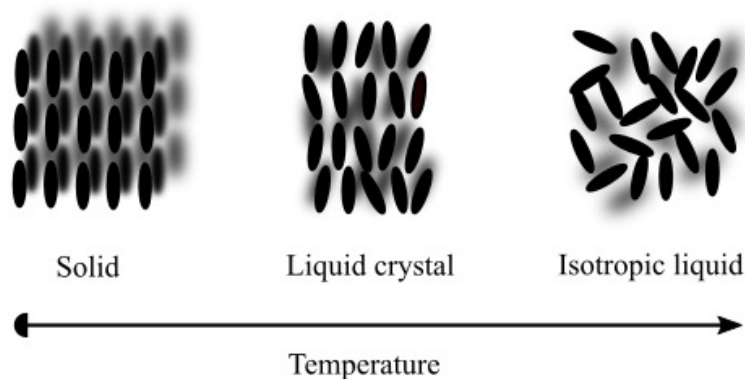


Figure 1.1 Schematic representation of varying state of molecule, which forms thermotropic phases with altered temperature.

On the other hand, LLCs can be obtained by dissolution of a surfactant molecule in an appropriate solvent, in general, water. Surfactant molecules are organic molecules and contain both hydrophilic and hydrophobic parts, Figure 1.2. These molecules aggregate to form the structure, so-called 'micelles', which are the building blocks of LLCs.

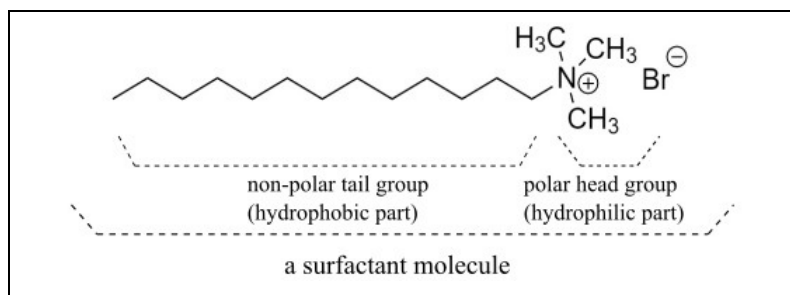


Figure 1.2 Molecular structure of a surfactant molecule. While the hydrophilic part is soluble in water, the hydrophobic part is not.

Unlike TLCs, fluidity of LLCs is granted by surrounding solvent molecules. LLCs are both concentration and temperature dependent mesophases and they have different structures, i.e. different kind of phases can be obtained by changing temperature and concentration of LLC samples.

As a worldwide comparison, LLCs are not as famous as TLCs, but they are becoming more important in daily life. Drug delivery systems, biotechnology, foods, cosmetics are some most common example areas of LLC phases (Lagerwall and Scalia, 2012; Engels and Rybinski, 1998). Besides, playing a role for a cell membrane in a body shows incontrovertible importance of this mesogen for human life. Therefore, it is obvious that all these applications, studies and developments excite scientists all over the world and triggers them to reveal hidden secrets about the LLCs.

1.1.1 Lyotropic Liquid Crystalline Structures

Lyotropic liquid crystals have different types of liquid crystalline structures caused by orientational orders of micelles with altering concentration and temperature conditions. Since this thesis is only related to the nematic phases, in the next section, information is given about these phases.

1.1.1.1 Lyotropic Nematic LC Phases (N)

Lyotropic nematic liquid crystals are comprised of finite size micelles that carry short-range positional and long-range orientational order. It is known that appropriate temperature and concentration changes in lyotropic liquid crystals lead to different orientation of micelles and micellar shapes. From this point of view, as a subclass of lyotropic liquid crystals, nematic liquid crystal phases can be classified according to their change in micellar shape with changing concentration and temperature. There are three types of nematic phases in literature as being discotic nematic phase (N_D), calamitic nematic phase (N_C) and biaxial nematic phase (N_B). Among these phases, both N_D and N_C phases are uniaxial and N_B phase is biaxial. Those phases are characterized by their well-known textures observed under polarizing optical microscope (Figure 1.3).

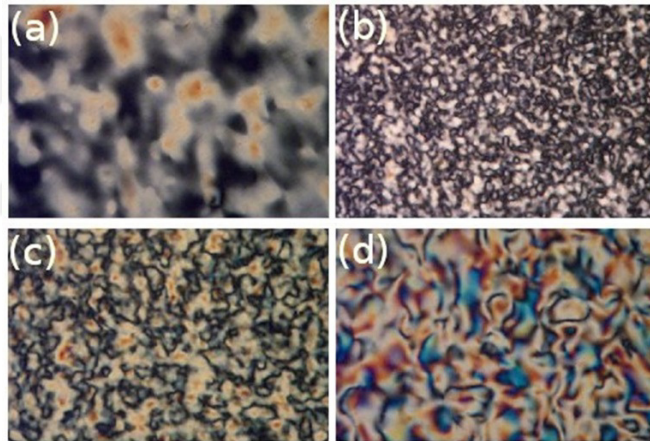


Figure 1.3 Characteristic textures for lyotropic nematic samples captured under polarizing optical microscope, where (a) N_D^- (b) N_B^- (c) N_B^+ (d) N_C^+ phases are shown. The (-) and (+) signs in the representation of the nematic phases correspond to the orientation of their optical axes with respect to the magnetic field direction (see part 1.1.1.2 for further information on the orientation of the optical axis of the nematic phases.)

The first lyotropic nematic phase was reported towards the end of the 1960s (Lawson and Flautt, 1967). In the following years, many studies were conducted to understand the properties of these phases. In these early studies, the existence of two types of nematic phases was determined and these phases were classified as Type I and Type II according to the direction of phase directors (optical axes) in the

magnetic field (Radley and Reeves, 1976; Radley and Saupe, 1978; Yu and Saupe, 1980a). It was proposed that the director of the Type I (Type II) phase prefers to align parallel (perpendicular) to the magnetic field direction. In the following years, Type I (Type II) phase was named as the N_C (N_D) one, assuming that Type I and Type II phases were considered to be composed of cylindrical-like and disc-like micelles (Radley and Saupe, 1978; Charvolin, 1979; Amaral, 1979, 1980; Neto and Amaral, 1980; Yu and Saupe, 1980a), respectively (Figure 1.4).

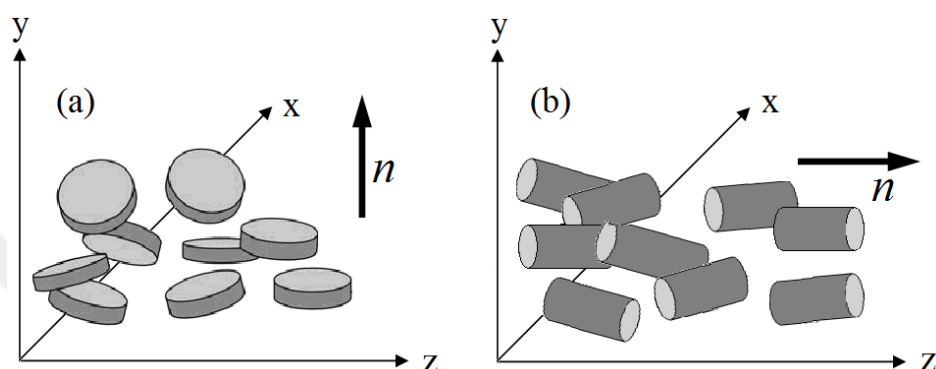


Figure 1.4 Orientations of (a) disc-like and (b) cylindrical-like micelles perpendicular and parallel, respectively, to magnetic field direction, H , along z . n (phase director or optical axis) represents the preferred alignment of the individual micelles with their local directors.

Freiser (1970, 1971) theoretically predicted N_B phase for the first time (Henriques, 1997; Severing, 2007; van den Pol, 2009; Nasrin, 2015; Sauerwein, 2016; Liu, 2018) after Taylor et al. (1970) reported a biaxial smectic C phase. His prediction was based on the orientations of two asymmetrical molecules, considering the interaction energy between them. However, at that time, there were no experimental results to support this theoretical prediction. Eventually, in 1980, Yu and Saupe (1980b) experimentally realized the evidence of the N_B phase for the first time in the ternary mixture of potassium laurate (KL)/decanol (DeOH)/ D_2O , where DeOH concentration was kept constant as 6.24 wt% and the weight concentration ratio of D_2O to KL changed from 2.67 to 2.56, via NMR and microscopic conoscopy studies (Figure 1.5). They constructed the partial phase diagram of this ternary mixture, depending on the concentration of the KL, and it was experimentally observed that N_B phase was an intermediate phase between other two uniaxial N_D and N_C phases. In 1985, Neto et al. (1985a) investigated the same ternary mixture in

more details. They used the experimental techniques optical microscopy, laser conoscopy and X-ray diffraction and found that the biaxial phase domain was relatively large ($\sim 15^\circ\text{C}$) for appropriate concentrations.

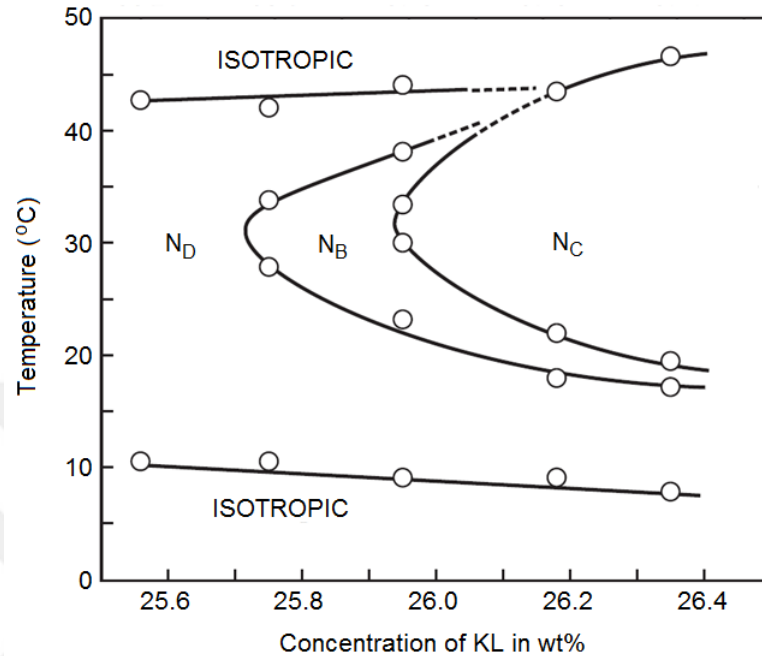


Figure 1.5 Phase diagram of KL/DeOH/water mixture which was constructed for the first time in the Ref (Yu and Saupe, 1980b).

In 1982, Bartolino et al. reported a partial phase diagram of a ternary mixture of sodium decyl sulfate (SdS)/DeOH/H₂O to contribute on the understanding of the biaxial nematic phases (Figure 1.6a). Their study was related to the optical observation on (a) the temperature dependence of the birefringence, Δn , and (b) the variation of the optical sign of oriented samples. They showed that, using phase compensator, uniaxial N_D (N_C) phase had positive (negative) birefringence (Figure 1.6b) and the phase transition from N_D to N_C exhibited a discontinuity passing through the biaxial phase.

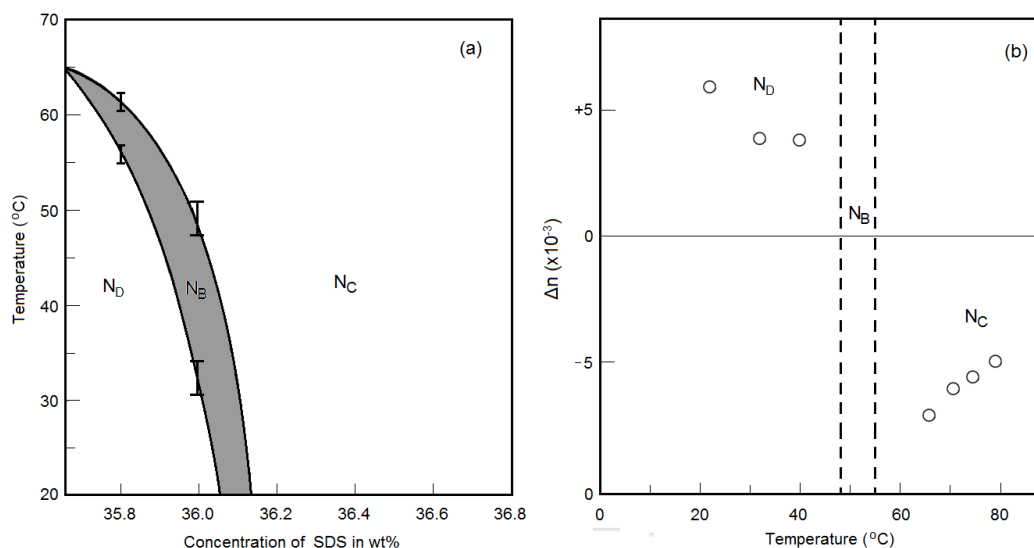


Figure 1.6 (a) Partial phase diagram of SDS/DeOH/water mixture given in the Ref (Bartolino, 1982). (b) The birefringences of the uniaxial nematic phases were for the sample of 35.8% SDS.

Finding the first biaxial nematic phase by Yu and Saupe not only proved the Freiser's prediction on the existing of that phase but also caused starting the discussions on the N_B phases in the literature (Yu, 1980a; Galerne, 1987; Madsen, 2004; Luckhurst, 2001; Acharya, 2004; Luckhurst, Nature, 2004; Galerne, 2006; Madsen, 2006; Dingemans et al., 2006; van del Pol, 2009). Some theoretical and computer simulation studies of binary mixtures of rod-like and disk-like rigid particles were reported in the literature (Straley, 1974; Biscarini, 1995; Camp, 1997; Taylor, 1991; Vanakaras, 2003; Berardi, 2008), most of which rejected the evidence of the N_B phase (Rabin et al., 1982; Stroobants, 1984; Chen, 1984; Hashim and Luckhurst, 1984, 1993; Pratibha, 1985,1990). It was suggested that the N_B phase arose from the coexistence of other two uniaxial N_D and N_C phases, as predicted by Alben (Alben, 1973). For instance, in 1984, considering Onsager theory, Stroobants and Lekkerkerker proposed a model where rod-like and disc-like particles coexist, giving rise to the biaxial nematic phase (Stroobants, 1984). They attributed their idea to "a mixture of disc-like and cylindrical-like micelles, MCD" model. However, some theoretical and experimental studies reported in the literature showed that the MCD type models had some problems to explain the existence of the N_B phases (Neto and Galerne, 2015). For instance, in 2000, Kooij and Lekkerkerker reported a very useful experimental study related to the liquid crystal phase behavior of mixed suspensions of rod- and platelike colloids and they proved that this type of mixture

shows demixing, i.e. the coexistence of rod- and platelike particles was not stable and the demixing results in the phase separation into an isotropic and uniaxial nematic phases (Kooij et al., 2000a).

In another study, Palffy et al. (1985) studied the phase behavior of the binary nematic liquid crystal mixtures in the absence of the external field by applying the Maier-Saupe mean field theory. They concluded that N_B phase was not thermodynamically stable phase with respect to other uniaxial N_D and N_C phases in the absence of the external field and the N_B phase would demix into two uniaxial ones. That is, N_B phase was a result of the coexistence of two uniaxial N_D and N_C phases, as predicted by MCD model, and the stabilization of N_B phase could be only achieved for some certain materials under external field condition. In a recent study, with a different approximation, Martinez-Raton et al. showed that demixing of rod-plate mixtures and the stability of the biaxial phase depend on aspect ratio and molar fraction of the rods (Martinez-Raton et al., 2016). However, Sharma et al. (1985) showed that there could be a possibility about the biaxial phase for being stable by increasing either the isotropic or the anisotropic parts of the interspecies interaction strength. The latter situation was also supported by some other theoretical studies, i.e. biaxial phases may be favored in multi-component (polydisperse) mixtures (Martinez-Raton, 2002) or by the attractive interactions (indeed, hydrogen bonding) between the unlike molecules (Vanakaras, 1997, 1998). However, for the symmetric (Varga, 2002a, 2002b, 2002c; Galindo, 2003) or asymmetric (Kooij, 2000a, 2000b, 2000c; 2001a, 2001b; Wensink, 2001, 2002) binary rod-plate mixtures, considering the stability of the biaxial phase with respect to demixing, the coexistence of rod-plate particles is not possible and the demixing is more favored, compared to the stability of these mixtures. From these respects, the demixing of the rod and platelike objects (in the case of the lyotropic systems, prolate or cylindrical-like and oblate or disc-like micelles do not coexist) requires the rejection of the MCD types model, as experimentally proved by Kooij and Lekkerkerker (Kooij, 2000a).

Although the discussions about the stability of the N_B phase were going on, experimentalist tried to find new lyotropic mixtures presenting the N_B phases. In 1985, Galerne et al. introduced a new ternary mixture of rubidium laurate (RbL)/DeOH/H₂O to the literature (Galerie et al., 1985). They investigated the

defect lines (disclinations) in both uniaxial and biaxial nematic phases and they observed that the disclination lines in the biaxial region made ‘zigzags’ while the uniaxial counterparts exhibited a ‘flexible’ behavior, i.e. the disclinations observed in the biaxial phase were different than those in the uniaxial ones, which may support the evidence of biaxial shape micelles in biaxial nematic liquid crystals.

Santos and Galerne investigated the uniaxial discotic nematic phase of KL/DeOH/D₂O by Rayleigh-scattering technique (Santos et al., 1984). They observed the dynamics of fluctuations of the biaxial order parameters close to the uniaxial-to-biaxial phase transition, at the side of the uniaxial phase, and showed that the micelles in the uniaxial discotic nematic phase exhibits the biaxial order.

However, until 1985, there was no any useful model to explain existence of the biaxial nematic phases. Eventually, a reliable and an important model was proposed by Neto (Neto, 1985b), which was also supported by Galerne (Galerne, 1987), for the N_B phases by rejecting the MCD types models. They investigated the uniaxial and biaxial nematic phases of the mixture KL/DeOH/D₂O by X-ray diffraction and observed that the micelles of three nematic phases, i.e. two uniaxials and one biaxial, are built up of biaxial platelets or pseudo-lamellar structure. This means that, in three nematic phases, the micelles are similar from the shape or geometry point of view. Their model, so-called “intrinsically biaxial micelles model, IBM”, is mainly based on two parameters: (a) micelle symmetry and (b) orientational fluctuations. According to the IBM model, the micelles have orthorhombic symmetry, (Figure 1.7a), in all three different nematic phases and the driving force for occurrences of these phases is ‘orientational fluctuations’. If we sketch micelles as an object of orthorhombic symmetry, as in Figure 1.7a, with typical dimensions A’, B’ and C’, we may choose the axes of the coordinate system, fixed in the micelles are α , β and γ . These orthorhombic micelles exhibit different orientational fluctuations for the formation of N_D, N_B or N_C phases. The orientational fluctuations around the axis 3 perpendicular to the largest micelle surface (along the symmetry axis γ) give rise to the formation of the N_D phase, (Figure 1.7b). In this situation, the micelle size A’ approximately equal to B’ (A’ ~ B’). By changing temperature to reach the transition from N_D to N_B, the micelle size along the symmetry axis α starts to be longer and the small amplitude orientational fluctuations along three axes (1, 2

and 3) lead to the formation of the N_B phase. If the temperature is changed until obtaining the N_C phase, the micelle size along α continues to be longer to favor the orientational fluctuations around the long micellar axis (parallel to the axis 1).

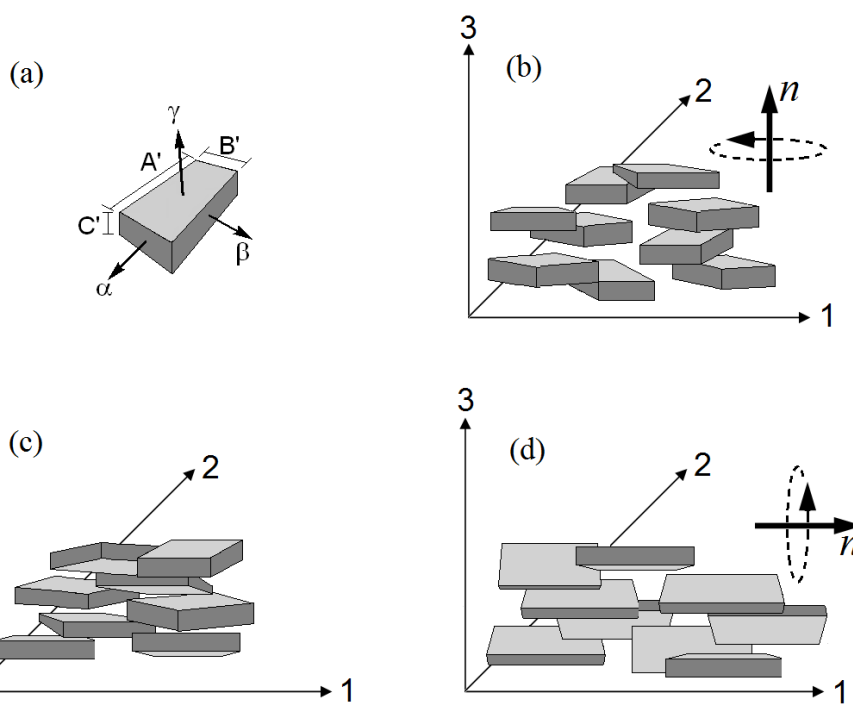


Figure 1.7 (a) Sketch of the orthorhombic micelle in the framework of the IBM model. The detergent amphiphilic bilayer is represented by C' . (b) N_D phase (c) N_B phase and (d) N_C phase.

A neutron scattering study was reported by Hendrikx et al. in 1986 and it supported to the IBM model from some respects (Hendrikx et al., 1986). In that study, the authors experimentally showed that the micelles of the N_C phase are statistically biaxial. They considered the uniaxial N_C phase as a made of prolate micelles. To do so, they modeled the micelles as an ellipsoid (Figure 1.8). This ellipsoid has three axes, being long (l), short (s) and intermediate (i) ones. The l -axis was chosen in the direction of the director and other axes (s and i) were in the normal section to the former one. For a prolate structure, the normal section of the ellipsoid should be circular, ($i=s$), which requires that it is isotropic. However, they observed from the neutron scattering experiments that the normal section was not circular and the micelles of the uniaxial phase in the vicinity of the uniaxial-to-biaxial phase transitions are statistically biaxial. This result indicated that there are no prolate or cylindrical-like micelles in the N_C phase as proposed by the IBM model.

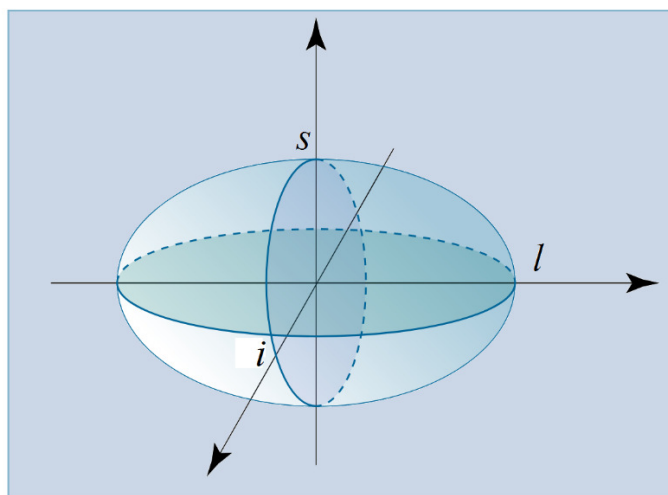


Figure 1.8 Schematic representation of an ellipsoid, which is a model aggregate for the N_C phase, with the three orthogonal axes, proposed in the Ref. (Hendrikx, 1986).

Until 1989, since the lyotropic mixtures exhibiting the biaxial nematic phases contained alcohol and surfactant, Oliveira et al. (1989) achieved to find a new mixture of KL/decylammonium chloride/water without alcohol. This new mixture was important because, as was suggested by Saupe et al. (Melnik, 1987), if a mixture has KL type surfactant and alcohol there is a possibility of a slow esterification in the mixture. In the study of the Ref. (Oliveira, 1989), the researchers investigated the mixtures of KL/DACl/water and KL/DeOH/water, i.e. alcohol free and with alcohol mixtures, respectively, to compare the physico-chemical stability of two types of the mixtures. Their long-term study was based on the birefringence and x-ray diffraction measurements. It was shown that the phase transition temperatures, birefringences and microscopic structures changed with time in the case of the mixtures including alcohol. However, for the alcohol-free mixtures, especially the x-ray diffraction results of the nematic phases stated that the alcohol-free mixtures were more stable than the one with alcohol.

In 1990, Vasilevyskaya et al. investigated two lyotropic mixtures exhibiting biaxial nematic phase (Vasilevyskaya, 1990). Since one of them, SdS/DeOH/H₂O, was already presented to the literature before by Bartolino (1982), other one, SdS/DeOH/H₂O/Na₂SO₄, was presented for the first time. Their experimental study was based on the measurement of the birefringences of the nematic phases depending on the temperature. They observed that this new system had much smaller

birefringences values with respect to the conventional lyotropic mixture KL/DeOH/H₂O (Yu, 1980b). As a result of their study, they concluded that the phase transitions from biaxial to uniaxials arise from the suppression of the rotation of the micelles around the axes. For instance, if the micelles turn around the short axis (long axis) of the micelle, it is possible to obtain the discotic (calamitic) nematic phase. In the case of the biaxial nematic, the rotation of the micelles is completely suppressed. Their conclusion is very similar to the IBM model. However, it is better to use the term “orientational fluctuations” instead of “suppression” to have different nematic phases as is suggested in the IBM model. In addition, in the case of the biaxial nematic, the rotations of the micelles or orientational fluctuations are not suppressed, instead, the orientational fluctuations with small amplitudes around the three symmetry axes of the orthorhombic micelles are responsible for the formation of the biaxial nematic phases.

Experimental studies and theoretical predictions stated that the biaxial nematic phase is an intermediate phase between two uniaxial nematic ones. Ho et al. (1991) reported an interesting study which was related to a new lyotropic mixture of sodium lauroyl sulfate/hexadecanol (HDeOH)/water, exhibiting a biaxial nematic phase in the case of diluted solutions. They obtained this biaxial phase after applying the sonication process on a gel-like phase. They showed surprisingly that a biaxial phase could not be an intermediate phase between two uniaxial nematics.

Another interesting study was published by Quist (1995) to investigate novel lyotropic mixture of sodium dodecylsulfate SDS/DeOH/H₂O via NMR spectroscopy. According to the Landau theory, the phase transitions from uniaxials-to-biaxial nematic phase transitions are second-order. However, Quist proposed that these phase transitions might be first-order. The author attributed the first-order N_D-N_B and N_B-N_C phase transitions to a variation in the aggregate (micelle) shape. This result is really very interesting, because other experimental and theoretical studies showed that the uniaxial-to-biaxial transitions have to be of second order. In addition, early (Neto, 1985a) and recent (Akpınar and Otluoğlu, 2016a; Akpınar and Canioz, 2018a) studies, especially obtained from the temperature dependence of the birefringences, showed that these phase transitions are of second order as predicted from mean-field theory (Freiser, 1970; Alben, 1973).

Since Quist (1995) reported two different biaxial nematic phase regions with positive and negative diamagnetic susceptibility anisotropy in the phase diagram, however, they did not study on the phase transitions between these N_{B+} and N_{B-} . This type of phase transition was investigated by de Melo Filho et al. (2003) in the novel lyotropic mixture of tetradecyltrimethylammonium bromide (TDTMABr)/DeOH/H₂O by measuring the deuterium quadrupolar splittings via Nuclear Magnetic Resonance. The results indicated that since the phase transition between N_{B+} and N_{B-} is first-order, the uniaxials-to-biaxial transitions are of second order in the agreement with the mean-field theory and in contrary with the Quist's study.

In 2009, van den Pol et al. reported very useful model system to experimentally realize biaxial phase in colloidal dispersions of boardlike particles (van den Pol, 2009). According to theory and simulations, the particles have the dimensions $L/W \approx W/T$, where L, W and T are length, width and thickness, Figure 1.9, to obtain a biaxial nematic phase (Alben, 1973; Straley, 1974; Camp, 1997) and they used goethite particles as a model system with $L/W=3.1$ and $W/T=3.0$. They examined the properties of the model system by small angle x-ray scattering under the effect of magnetic field, i.e. they studied with well-oriented system. Their results indicated the evidence of the biaxial nematic phases. Indeed, their model system shown in Figure 1.9, is similar to what is proposed by the IBM model in terms of the micelle shapes and, from this respect, the study of the Ref. (van den Pol, 2009) supports the IBM model.

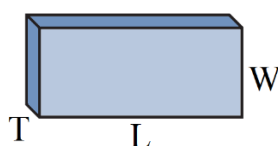


Figure 1.9 Schematic representation of shape of a goethite particle.

As we have reviewed some important studies on lyotropic nematic phases above, while some studies reject the existence of the biaxial phase, others strongly assert that the biaxial phase is a thermodynamically distinct stable phase such as uniaxial ones with theoretical approximations and experimental results. Indeed, these controversies arise from the absence of enough amount of lyotropic mixtures in the literature and thermotropic counterpart is due to not yet found. In addition, the

factors that affect the formation of the nematic phases, especially biaxial one, have to be found. Some recent studies have shown that alkyl chain lengths of both surfactants and long chain alcohols, kosmotrope and chaotrope properties of counterions and ions, and localization of dopant molecules at the micelle surfaces play important roles on the stabilization of different nematic phases.

1.1.1.2 Optical and Magnetic Properties of Nematic Phases

One of the most important property of liquid crystals is that they are anisotropic materials like solids. When a polarized light beam is passed through a liquid crystalline sample, it splits into two plane-polarized rays (ordinary and extraordinary) with different velocities, i.e. with two different refractive indices, n_o and n_e , respectively. Electric vectors of the ordinary and extraordinary rays vibrate in different directions with respect to the optical axis of the liquid crystal phase. The direction is perpendicular or parallel to the optical axis. Because the electric vector of the ordinary (extraordinary) ray is perpendicular (parallel) to the optical axis, n_o (n_e) is also shown as n_{\perp} (n_{\parallel}), i.e. $n_o=n_{\perp}$ ($n_e=n_{\parallel}$). The difference between these two refractive indices is known as double refraction or birefringence, $\Delta n=n_e-n_o=n_{\parallel}-n_{\perp}$, and it plays an important role on the electrooptical applications of the liquid crystals. In the case of $n_{\parallel}>n_{\perp}$ ($n_{\parallel}<n_{\perp}$), the optical anisotropy of the sample is greater (smaller) than zero, i.e., for instance, a lyotropic nematic phase has positive (negative) birefringence. The N_D and N_C phases are described by positive and negative birefringence ($\Delta n>0$ and $\Delta n<0$), respectively. The sign of optical anisotropy can be easily determined from conoscopic investigation of well-aligned nematic samples, Figure 1.10, under polarising optical microscopy with Bertrand lens and $\frac{1}{4}$ retardation plate (Figure 1.11).

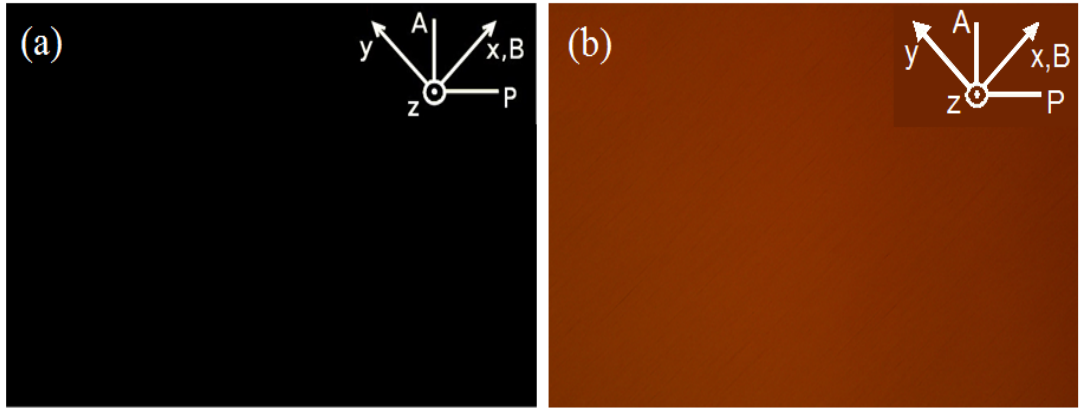


Figure 1.10 A well-aligned texture of uniaxial (a) N_D (homeotropic alignment) and (b) N_C (planar alignment) phases. A: analyzer; P: polarizer; B: magnetic field direction; x, y and z are the laboratory frame axes.

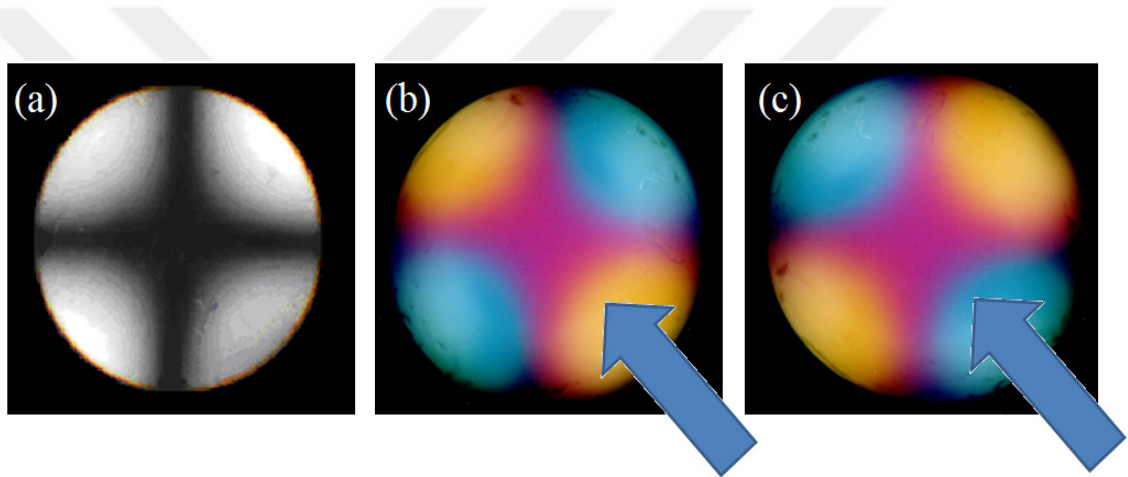


Figure 1.11 (a) The conoscopic investigations of well-aligned textures of uniaxial nematic phases, which show characteristic cross dark brushes. An interference figure, i.e. cross dark brushes, indicates a perfect alignment of the optical axis of a nematic phase. Interference colors of nematic phases for (b) $\Delta n > 0$ and (c) $\Delta n < 0$ as a $\frac{1}{4} \lambda$ retardation plate is inserted in the light path of the polarizing light microscope. Blue arrows represent the direction of the plate.

Alignment of the optical axis of the nematic phases with respect to the applied magnetic field is another important property to describe them. Liquid crystals are known to be diamagnetic materials. The magnetization of diamagnetic materials is proportional to the magnetic field strength, B , and the magnetic susceptibility, χ , via the following equation

$$M = \chi H \quad (1.1)$$

Notice that for diamagnetic materials χ is always negative.

Two different components of diamagnetic susceptibilities with respect to the magnetic field direction are defined for nematic phases. The optical axis of the nematic phase can be either parallel to the applied magnetic field, $\chi_{//}$, in the perpendicular direction to the magnetic field, χ_{\perp} . The difference between these two components of diamagnetic susceptibilities, $\chi_{//} - \chi_{\perp}$, of the nematic phase is known as the diamagnetic susceptibility anisotropy, $\Delta\chi$, of a liquid crystalline sample (in our case, lyotropic nematic phases). In the case of $\chi_{//} > \chi_{\perp}$, a liquid crystalline sample has a positive diamagnetic susceptibility anisotropy ($\Delta\chi > 0$) and the optical axis of the liquid crystal sample aligns parallel to the direction of applied magnetic field. Inversely, when $\chi_{//} < \chi_{\perp}$, the diamagnetic susceptibility anisotropy is negative ($\Delta\chi < 0$) which means that the direction of the optical axis is perpendicular to the direction of magnetic field. If $\chi_{//} = \chi_{\perp}$, the diamagnetic susceptibility anisotropy is equal to zero, i.e. the system is isotropic.

In addition to the optical anisotropy (Δn), the sign of the diamagnetic susceptibility anisotropy is also a criterion for characterization of nematic phases. In general, Δn and $\Delta\chi$ have opposite signs. If the optical axis of a nematic liquid crystal sample aligns perpendicular (parallel) to an applied magnetic field, $\Delta\chi < 0$ ($\Delta\chi > 0$) but $\Delta n > 0$ ($\Delta n < 0$). The former and latter cases correspond to the uniaxial N_D and uniaxial N_C phases, respectively, and they are characterized by their well-aligned homeotropic (N_D , Figure 1.10a) and planar (N_C , Figure 1.10b) textures under polarizing optical microscopy under the effect of applied magnetic field. In terms of the sign of the $\Delta\chi$, the N_D (N_C) phase is labelled as N_D^- and N_C^+ .

From the diamagnetic susceptibility anisotropy point of view, considering the diamagnetic susceptibilities along three two-fold symmetry axes being χ_{33} , χ_{22} and χ_{11} , the biaxial nematics are identified with positive and negative $\Delta\chi$, N_B^+ and N_B^- . For the biaxial nematics, the diamagnetic susceptibility anisotropy is defined as:

$$\Delta\chi = \chi_{33} - \frac{\chi_{11} + \chi_{22}}{2} \quad (1.2)$$

In the case of $\Delta\chi>0$ ($\Delta\chi<0$), the largest (smallest) diamagnetic susceptibility is larger (less) than the average of the diamagnetic susceptibilities of other axes and the biaxial phase aligns parallel (perpendicular) to the magnetic field direction (Quist, 1995; Melo Filho et al., 2003). Two different biaxial nematic phase regions with positive and negative diamagnetic susceptibility anisotropies (N_B^+ and N_B^- , respectively) on the phase diagram were reported (Quist, 1995). From NMR studies, it was proved that the phase transition from N_B^+ to N_B^- is first-order (Melo Filho et al., 2003).

1.2 As a Precursor of Lyotropic Nematic Phases: Isotropic Micellar Solutions

As mentioned in previous sections, micelles formed by the aggregation of surfactant molecules are building blocks of lyotropic liquid crystals. According to the literature, some parameters, which can be obtained from isotropic micellar solutions, take a supportive role to understand properties of lyotropic structures better (Dawin et al., 2009; Akpınar, 2016b; Akpınar, 2018b).

Descriptively, surfactants are organic molecules that change surface tension in water. In their detailed structure, they show dual affinity to any kind of solvent with its hydrophilic (polar) head group part and hydrophobic (nonpolar) organic tail part. Although, changes in both polar and nonpolar parts lead to obtaining variety of surfactant types, the main classification can be done according to charge carried by head group of the surfactant as anionic, cationic, nonionic and zwitterionic.

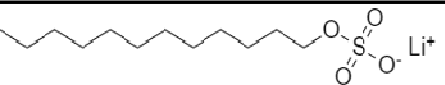
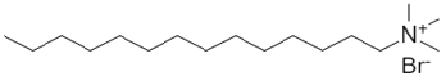
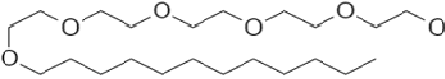
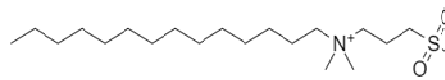
Type of Surfactants	Example molecule	Molecular Structure
Anionic	Lithium dodecyl sulfate	
Cationic	Tetradecyltrimethylammonium bromide	
Non-ionic	Pentaethylene glycol monododecyl ether	
Zwitterionic	N-tetradecyl-N,N-dimethyl-3-ammino-1-propanesulfonate	

Figure 1.12 Classification of surfactant types and their corresponding surfactant molecule examples.

When surfactants are dissolved in water, hydrophobic group of the surfactant leads to an increase in the free energy of the system by disrupting water structures. To minimize this emerging energy, surfactant molecules produce a thin layer until the surface of the solution is saturated. After saturation process takes place at the surface, surfactant molecules forms clusters in order to provide continuation for minimizing liberated free energy and balance. This exact concentration at which surfactant molecules start to aggregate and generate more complex units, so-called micelles, is critical micelle concentration (cmc) (Shinoda, 1963).

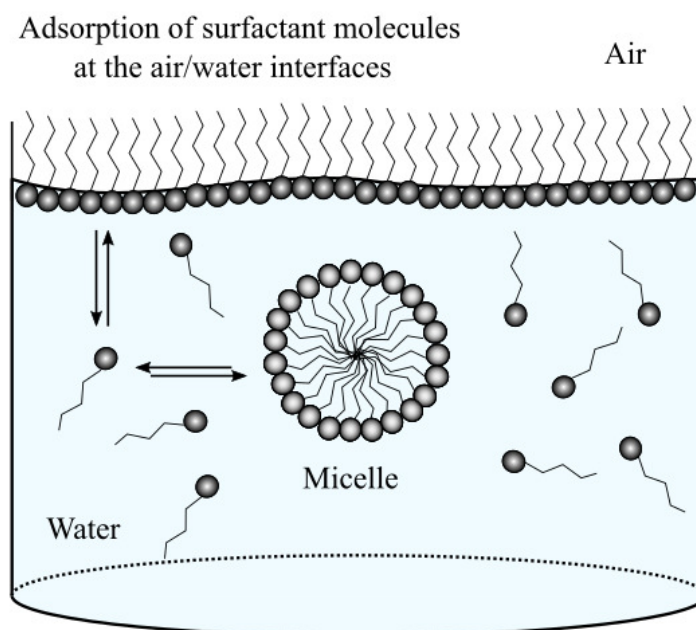


Figure 1.13 Schematic representation of micelle formation via dynamic equilibrium among air/water interface adsorbed surfactant monomers, surfactant monomers in water and micelles.

From formation point of view, micelles are always in kinetic process and they are exposed to continuous association and dissociation processes (Aniansson, 1976). After arrival of critical micelle concentration, number of surfactant monomer remains constant with increasing surfactant concentration for a mixture by forming new micelles for system.

All surfactant molecules have their unique and characteristic critical micelle concentration values. Critical micelle concentration can be determined from some methods, where sharp physical changes occur at cmc from their concentration-based measurements (Figure 1.14).

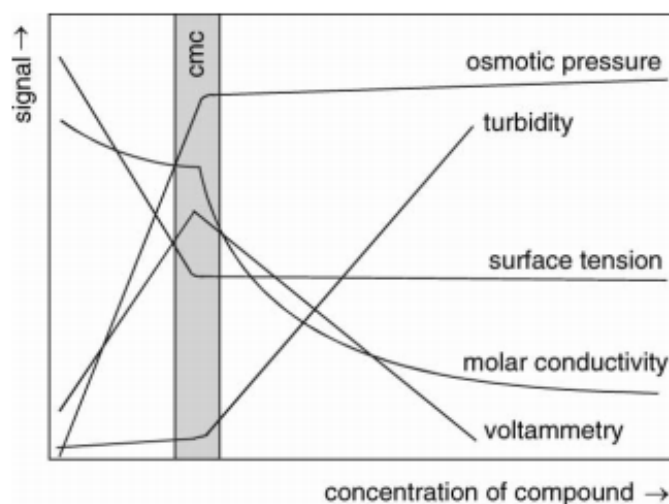


Figure 1.14 Representation of methods used for critical micelle concentration (Nesměrák, 2006).

1.2.1 Thermodynamic Parameters of Micellization

In an appropriate solvent, all surfactant molecules show different physical properties after critical micelle concentration. Scientists working on this field benefit from thermodynamic parameters to identify micellization process, side effects of additives, stability of micelles and spontaneity of formation of micelles. One of the common method to determine thermodynamic parameters is conductivity measurements. Having sharp break at cmc value for conductivity (κ) vs concentration graph provides to calculate degree of ionization of counterions (α) and

degree of counterion binding (β). While ratio of linear slopes for both before and after cmc regions gives the degree of ionization ($\alpha=S_2/S_1$), then the degree of counterion binding can be found from $\beta=1-\alpha$.

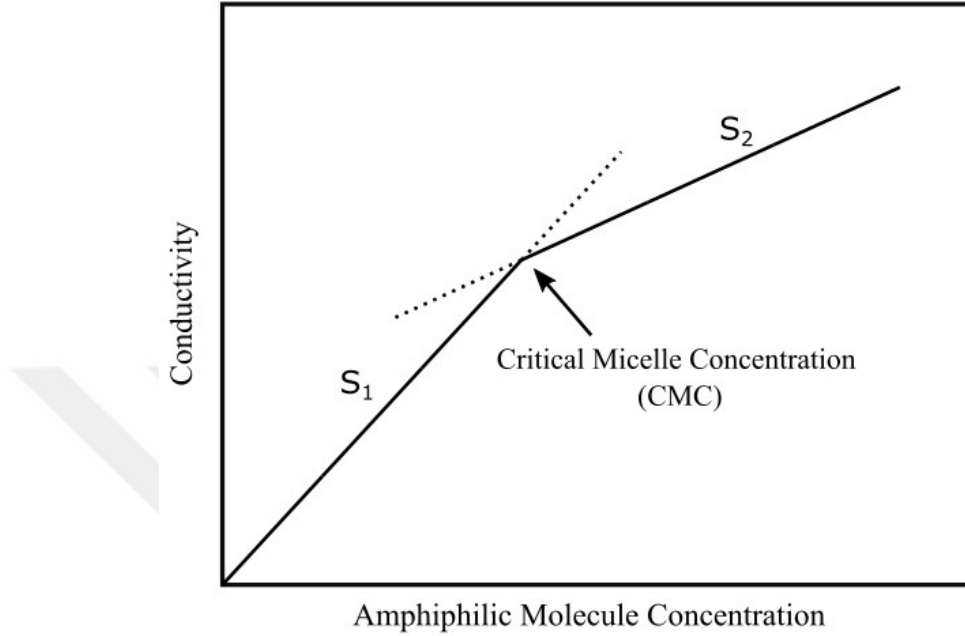


Figure 1.15 Conductivity vs concentration plot where S_1 and S_2 terms indicates the slopes before and after critical micelle concentration, respectively.

In ionic surfactant systems, temperature dependent thermodynamic parameters, standard Gibbs free energy of micellization ($\Delta_{mic}G^\circ$), standard enthalpy of micellization ($\Delta_{mic}H^\circ$) and standard entropy change ($\Delta_{mic}S^\circ$), are derived from the degree of counterion binding value as follows:

$$\Delta G_{mic}^\circ = (1 + \beta)RT \ln X_{cmc} \quad (1.3)$$

$$\Delta H_{mic}^\circ = -(1 + \beta)RT^2 \left(\frac{\partial \ln X_{cmc}}{\partial T} \right) \quad (1.4)$$

$$\Delta S_{mic}^\circ = \frac{(\Delta H_{mic}^\circ - \Delta G_{mic}^\circ)}{T} \quad (1.5)$$

where R and X_{cmc} refer ideal gas constant and mole fraction of surfactant at the cmc, respectively.

2. AIM AND SCOPE OF THE STUDY

Lyotropic nematic liquid crystals have been investigating for several years to clarify their stabilization mechanisms. Early studies about the orientation of the director of uniaxial nematic phases subjected to external magnetic fields showed that it depends on the shapes and symmetry of the micelles. For instance, in uniaxial discotic (calamitic) nematic phase, N_D (N_C), local directors exhibit preferred alignment in the perpendicular (parallel) direction with respect to the magnetic field. However, after the discovery of biaxial nematic phase in 1980 (Yu and Saupe, 1980b), N_B , as an intermediate phase between the two uniaxial ones, the studies on the uniaxial-to-biaxial nematic phase transitions showed that those phase transitions are of second order (Galerne et al., 1983; Braga et al., 2016) as predicted by a Landau-type mean-field theory (Freiser, 1970; Alben, 1973). From the symmetry point of view, this indicates the occurrence of continuous modifications on the dimensions of the same kind (symmetry) of micelles.

There are in the literature still controversies about the stabilization mechanism of lyotropic nematic phases. Indeed, these controversies arose from the stability of biaxial nematic phase. Some authors claimed the occurrence of the biaxial nematic phase as a result of the coexistence of two uniaxial phases (Stroobants and Lekkerkerker, 1984), however, without strong evidences to support this claim. In contrast, other scientists asserted that the biaxial nematic phase is a distinct thermodynamically stable phase (Akpınar, 2012a, 2018a; Bartolino et al., 1982; Filho et al., 2003).

More recently, Akpınar and Neto (2012b, 2015, 2016b, 2018a) reported on how the choose of the surfactants, co-surfactants, electrolytes and relative concentrations of the mixture constituents play a significant role on the stabilization of the different nematic phases, in particular the biaxial one. Depending on the lyotropic phase desired, co-surfactants and/or electrolyte may be added into the surfactant/water mixture. They investigated the effects of: a) the alkyl chain length of both surfactant and alcohol molecules (Akpınar et al., 2012b, 2018a), and b) the

specific interactions between the ionic species, surfactant head groups and ions of electrolytes, at the micelle surfaces (Akpinar et al., 2015, 2016b) on the stabilization of the nematic phases. For instance, while the strong (weak) interactions between the surfactant head groups and electrolyte ions give rise to the formation of N_D (N_C) phase, it is possible to obtain N_B phase in the case of the intermediate level of those interactions at micelle surfaces. Of course, these different interactions change the curvature of the micelle surfaces causing different packing geometry of the surfactant molecules in the micelles.

Since the basic units of both lyotropic liquid crystals and isotropic (dilute) micellar solutions are micelles, they have some similar properties. One of the most common properties is that if an electrolyte is added to the solutions, micelles grow in both solutions by changing the packing geometry of the surfactants (Akpinar et al., 2016a; Israelachvili, 1991; Dawin et al., 2009). Many studies reported in the literature showed that the presence of the electrolytes in isotropic micellar solutions changes the micelle shapes from sphere to rod or lamellae or disk in the case of direct micelle. This change is followed by packing parameter of the surfactants in the isotropic micellar solutions. Dawin et al. (2009) reported that the packing parameter also gives useful information about the stabilization of lyotropic phases. They evaluated the change in the packing parameter from isotropic-to-nematic phase (T_{NI}) to nematic-to-lamellar (T_{NL}) phase transitions. They observed that the packing parameter increases from T_{NI} to T_{NL} , as observed in isotropic micellar solutions. Consequently, the information obtained from isotropic micellar solutions may be applied to lyotropic nematic phases (Akpinar et al., 2016a; 2018b).

The change of the micelle curvature by addition of electrolyte into the micellar solutions is well-known in the literature. Indeed, this effect arises from how the ionic species form ion pairs at the micelle surfaces. In other words, the interactions at micelle surfaces modify the micelle shapes by changing the packing of the surfactants.

Now, the question is how can we modify the curvature of the micelle surfaces at constant electrolyte concentration to obtain different lyotropic nematic phases, or other phases such as lamellar or hexagonal? An alternative way may be the modification of the surfactant head groups. To do so, we synthesized some surfactant molecules, tetradecylalkylammonium bromides, providing the symmetric and asymmetric head-group growth. By this way, we change the strength of the

interactions between the head groups and the ions (counterions of the surfactants and/or ions of electrolytes).

In this study, we aimed to see the effect of head-group growth of the surfactants to stabilize different lyotropic nematic phases. Thus, researchers may decide which surfactant should be chosen to obtain the lyotropic biaxial nematic phase. The experimental design of this study is: in the first part, we examined the lyotropic liquid crystalline properties of mixtures with tetradecylalkylammonium bromides by means of laser conoscopy and polarizing optical microscope; in the second part, we studied the isotropic micellar solutions of those surfactants by electrical conductivity; then, we combined all results to understand the role of symmetric and asymmetric head-group growth on the stabilization of the different lyotropic nematic phases.

3. MATERIALS AND METHODS

3.1 Chemicals

All chemicals used in this work were purchased from Sigma, Merck and Aldrich in high purities (>99%). Except tetradecyltrimethylammonium bromide, commercially available, tetradecylalkylammonium bromides (tetradecyldimethylammoniumbromide, TDMABr; tetradecyldimethylethylammonium bromide, TDMEABr; tetradecyldiethylmethylammonium bromide, TDEMABr; tetradecyltriethylammonium bromide, TTEABr; tetradecyltripropyl-ammonium bromide, TTPrABr; tetradecyltributylammonium bromide, TTBuABr) synthesized by a procedure taken from literature (Buckingham et al., 1993). The molecular structures of tetradecylalkylammonium bromides are given in Figure 3.1 According to the procedure, quaternary ammonium bromide surfactants were prepared by limiting reaction of 1-bromotetradecane with the alkyl amines. Stoichiometrically calculated amounts of the reactants were placed into reflux system for approximately 48 hours in ethanol solvent. During the reaction goes on, reaction mixture was controlled with TLC method to understand completion. Then, yellow two-phase mixture was obtained in reaction flask and it was rotary-evaporated to remove ethanol. The mixture was treated with cold diethyl ether solution and placed into a freezer to obtain product as a crystal. Afterwards, the mixture was filtered, and the product was dried under the vacuum to remove solvent traces. Finally, all synthesized surfactant molecules recrystallized with chloroform and diethyl ether at least three times. The products were characterized by FT-IR (Figures 3.2-3.10).

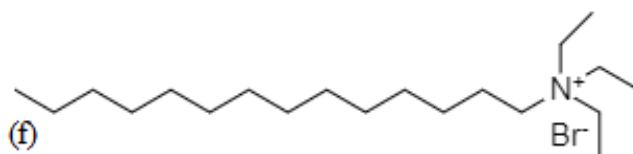
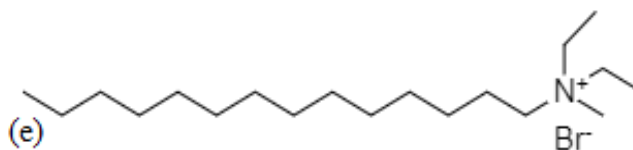
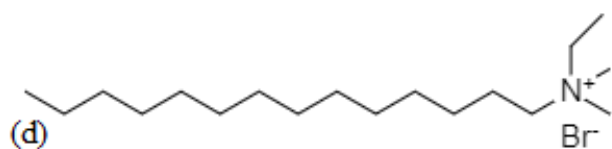
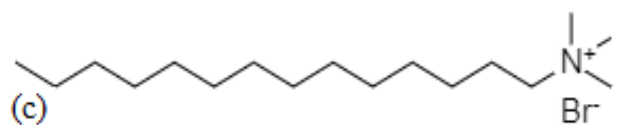
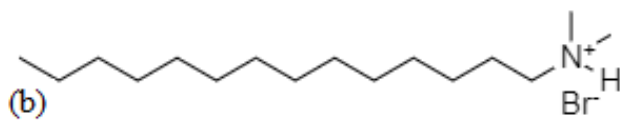
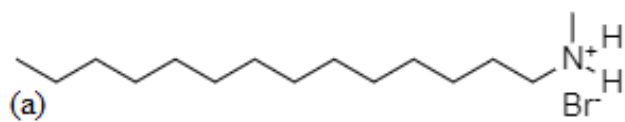


Figure 3.1 Molecular structures of tetradecylalkylammonium bromides

- (a) tetradecyldihydrogenmethylammonium bromide,
- (b) tetradecyldimethylhydrogen-ammonium bromide,
- (c) tetradecyltrimethylammonium bromide,
- (d) tetradecyldimethylethylammonium bromide,
- (e) tetradecyldiethylmethylammonium bromide,
- (f) tetradecyltriethylammonium bromide.

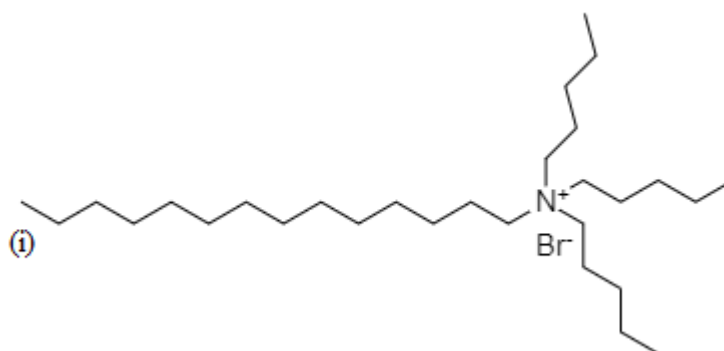
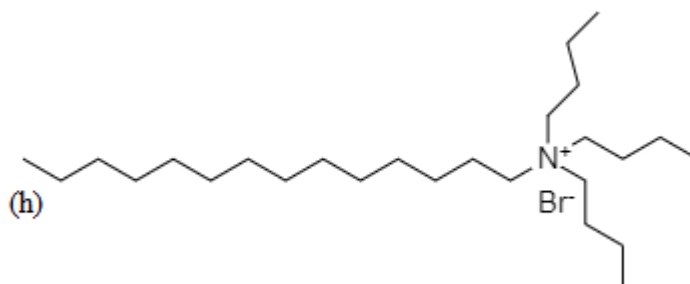
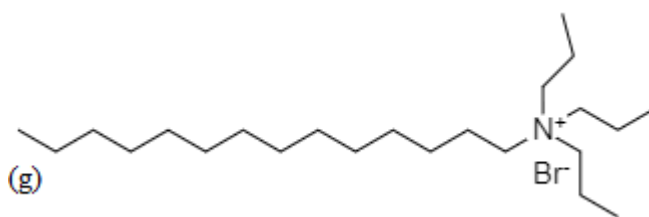


Figure 3.1 (continued) Molecular structures of tetradecylalkylammonium bromides (g) tetradecyltripropylammonium bromide, (h) tetradecyltributhylammonium bromide, (i) tetradecyltripentylammonium bromide.

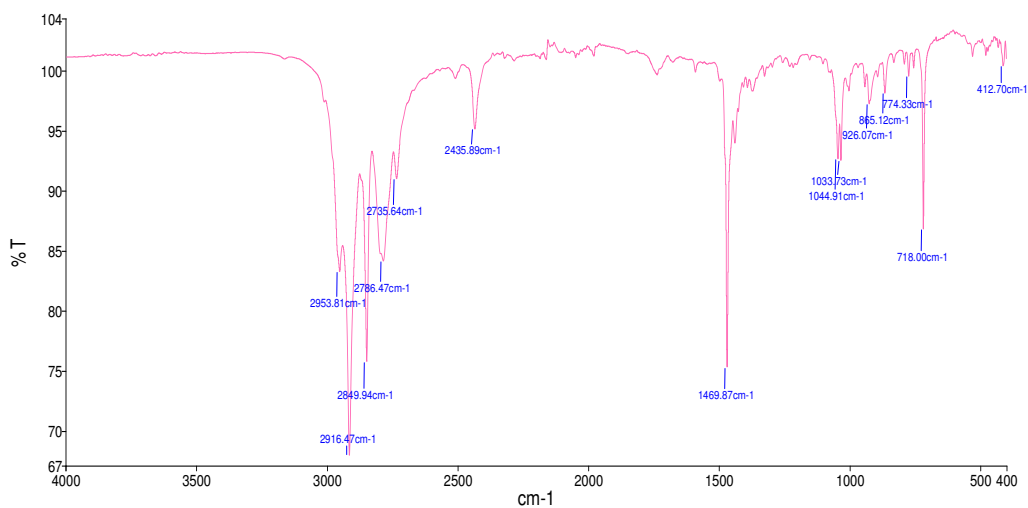


Figure 3.2 FT-IR spectroscopy of tetradecyldihydrogenmethylammonium bromide molecule.

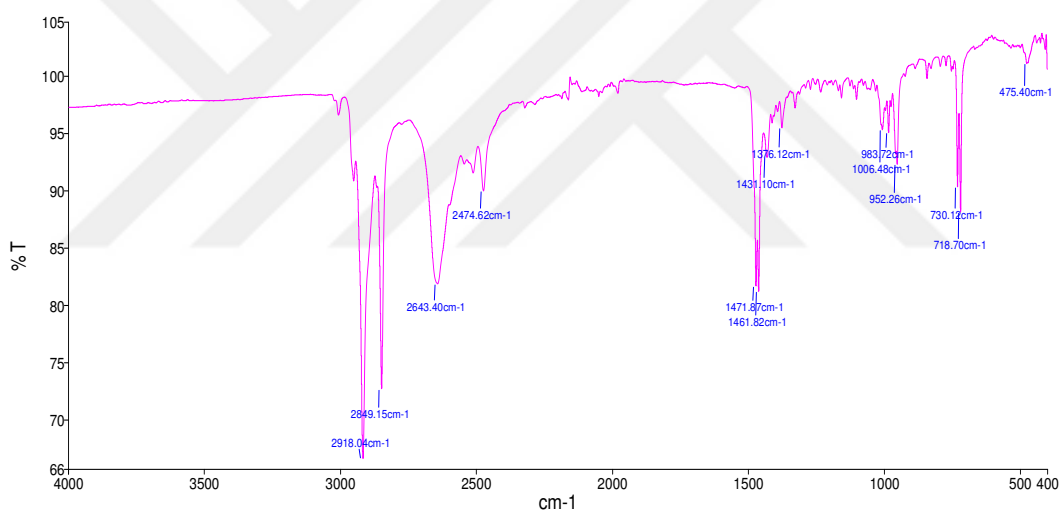


Figure 3.3 FT-IR spectroscopy of tetradecyldimethylhydrogenammonium bromide molecule.

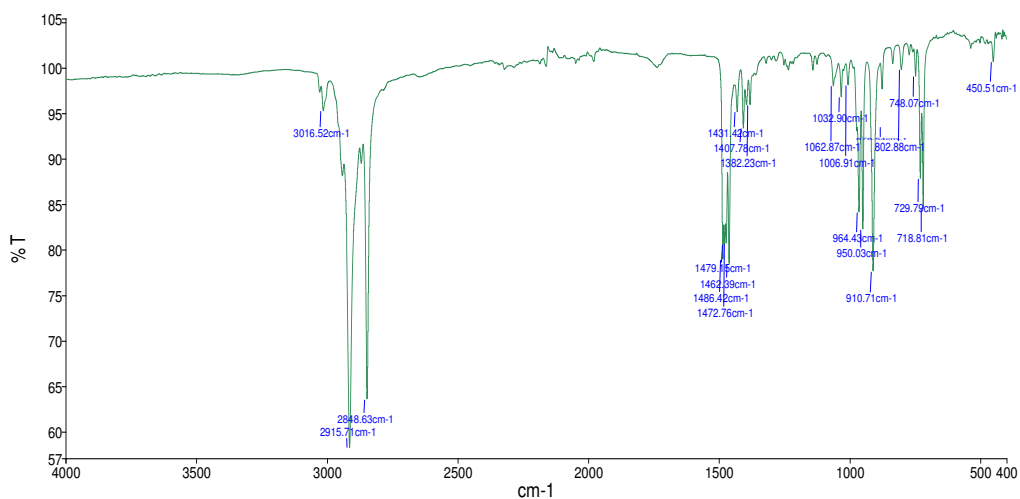


Figure 3.4 FT-IR spectroscopy of tetradecyltrimethylammonium bromide molecule.

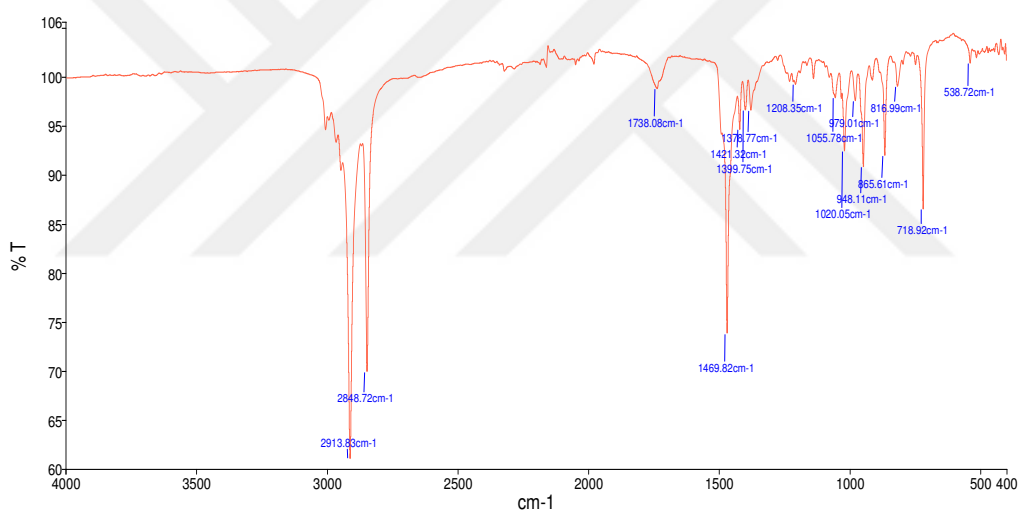


Figure 3.5 FT-IR spectroscopy of tetradecyldimethylethylammonium bromide molecule.

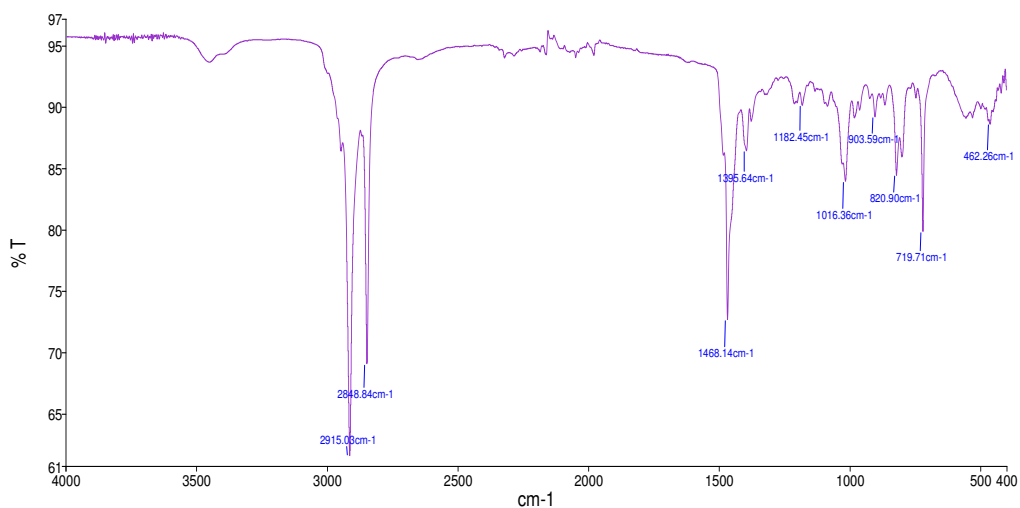


Figure 3.6 FT-IR spectroscopy of tetradecyldiethylmethylammonium bromide molecule.

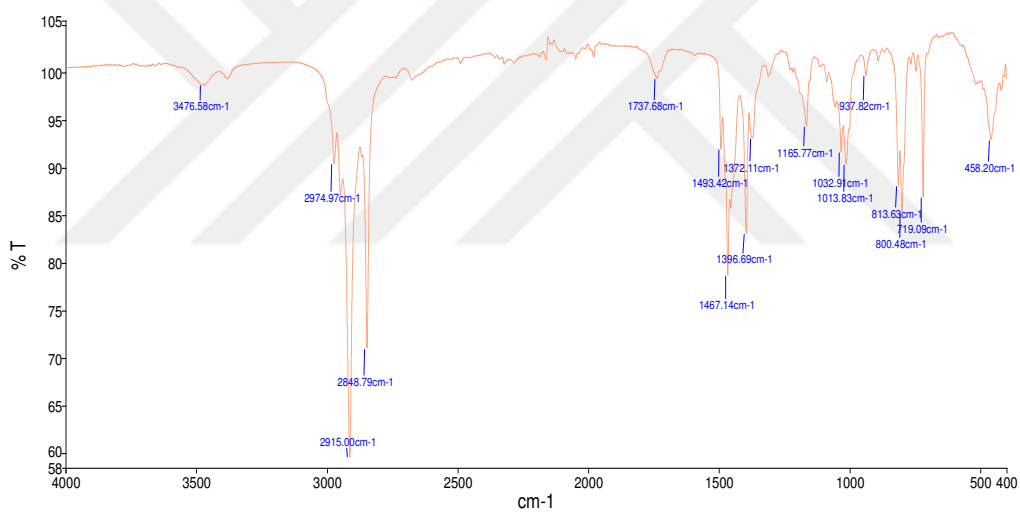


Figure 3.7 FT-IR spectroscopy of tetradecyltriethylammonium bromide molecule.

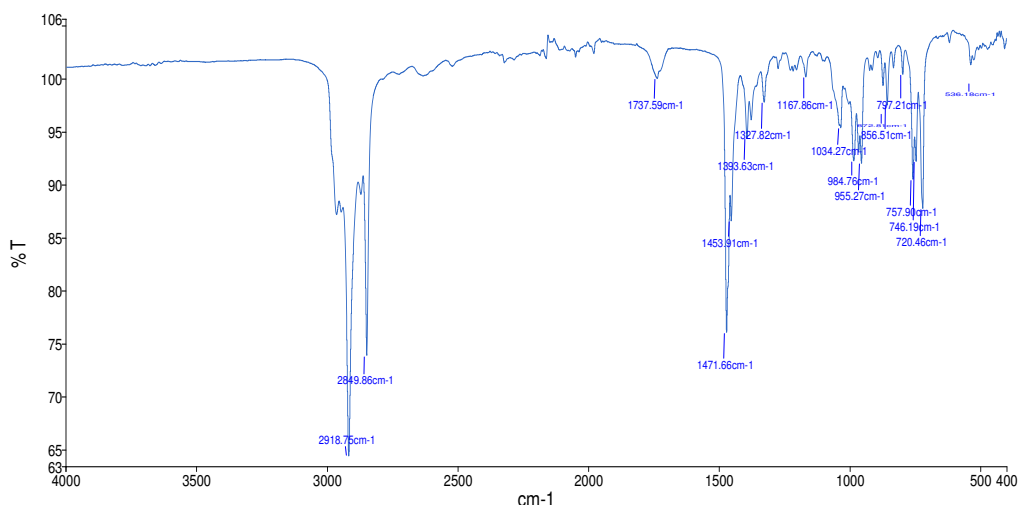


Figure 3.8 FT-IR spectroscopy of tetradecyltripropylammonium bromide molecule.

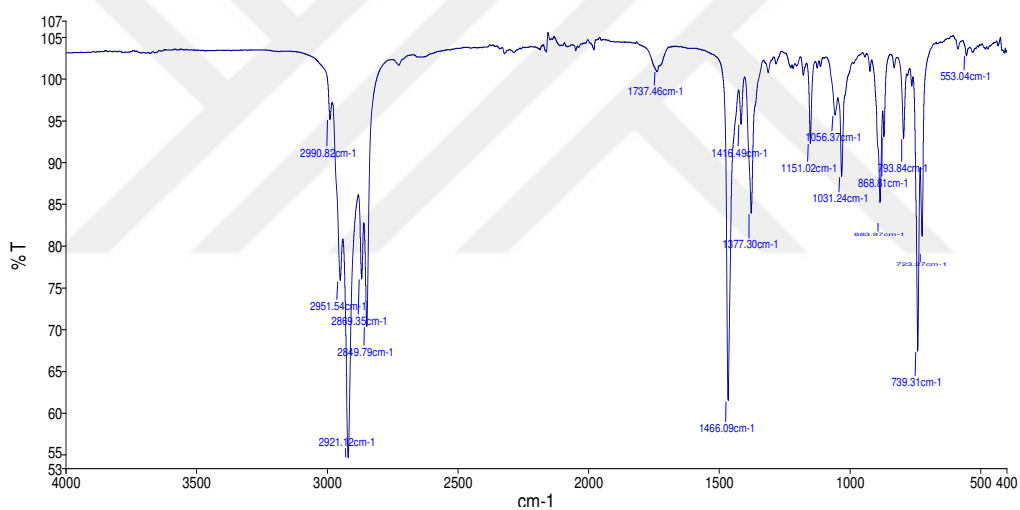


Figure 3.9 FT-IR spectroscopy of tetradecyltributylammonium bromide molecule.

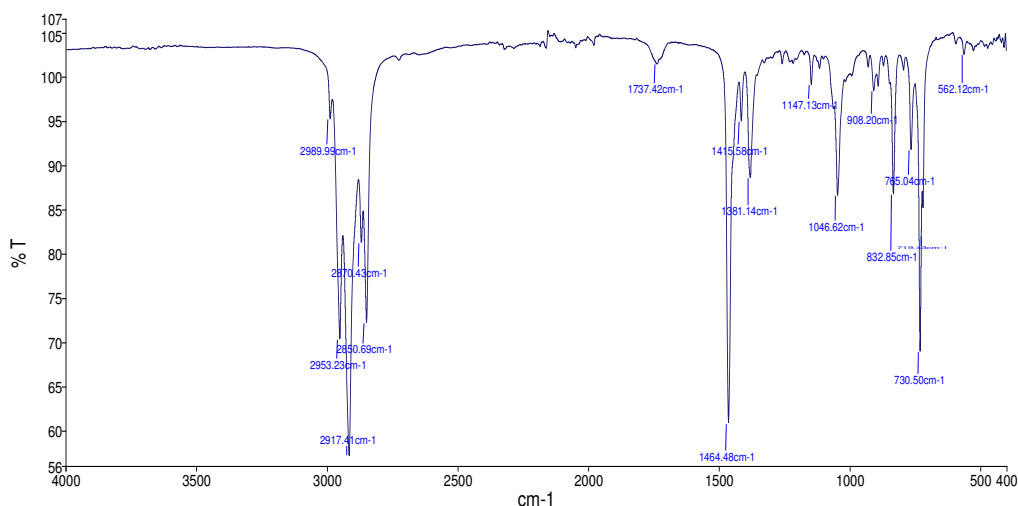


Figure 3.10 FT-IR spectroscopy of tetradecyltripentylammonium bromide molecule.

3.2 Electrical Conductivity

Conductivity measurements were performed with a Mettler-Toledo-S470 Seven Excellence pH/conductivity meter at 30°C. A dip-type glass conductivity cell was inserted in an aluminum holder, in which water was circulated to obtain stable temperature. Water circulation was provided by Polyscience SD070R water circulator granted desired temperatures with 0.1°C precision. The cell constant value measured as 1.03 cm⁻¹ with known concentrations of KCl solutions.

In order to determine the critical micelle concentrations of the surfactants, isotropic micellar solutions were used. The surfactant stock solutions with known concentration were prepared by dissolving surfactant molecules in ultra-pure water provided by Millipore Direct-Q3 UV. Each stock solution was added to ultra pure water in the conductivity cell with an Eppendorf micropipette until the concentration of solution exceeds to 2 or 2.5 times the critical micelle concentration. All the measurements repeated at least three times to minimize the experimental error in the measurements.

3.3 Preparation Process of Liquid Crystal Samples

As mentioned before, lyotropic liquid crystals are concentration dependent mesophases. One of the most important issue about preparing these solutions is a weighing procedure. In this stage, the weighing procedure carried out with 5-digit balance (Radwag AS82/220.R2) into test tubes with screw cap and then sealed with parafilm to prevent water loss from the test tubes. After completion of weighing process, homogenization of solution was ensured by performing vortex (Velp TX4 with IR sensor) and centrifuge (Hettich EBA20) operations until the homogeneous solution was obtained. After homogenization process, water based ferrofluid was added (1 μ L for 1 g sample) to the homogeneous solution to get well-oriented nematic samples in magnetic field (\sim 2.3 kG, checked with Lakeshore 475 Model Gaussmeter) (Akpinar, 2012a and 2012b; Neto et al., 2005).

3.4 Laser Conoscopy

If the laboratory frame axes are chosen with two axes (1 and 2) parallel to the A'-B' (Figure 1.7) plane and axis 3 normal to the biggest surface of the sample, three different refractive indices are defined as n_1 , n_2 and n_3 . There exist three different possibilities in terms of the relative values of the those refractive indices, where $n_1 \leq n_2 \leq n_3$. In the first case, three refractive indices are equal to each other, $n_1 = n_2 = n_3$, which indicates that the sample is isotropic, and the indicatrix is a sphere (Figure 3.11a). For an anisotropic sample, like thermotropic or lyotropic liquid crystals, the refractive indices are not equal to each other and the indicatrix is an ellipsoid (Figure 3.11b and 3.11c). In the case of thermotropic uniaxial nematic phases,

$$n_1 = n_2 \leq n_3 \text{ (prolate ellipsoid)}$$

or

$$n_1 \leq n_2 = n_3 \text{ (oblate ellipsoid)}$$

Because the refractive index along (in plane perpendicular to) the optical axis of the nematic phase corresponds to the refractive index of the extraordinary ray, n_e (n_o), $n_3 = n_e$ and other two refractive indices are the refractive indices of the ordinary rays, $n_1 = n_2 = n_o$. Thus, the birefringences, $\Delta n = n_e - n_o$, of thermotropic nematic phases,

where, in general, rod-like molecules are their structural units and the molecular long axis is parallel to the optical axis of the nematic phase, are positive ($\Delta n_{32}=n_3-n_2>0$, Figure 3.11) and negative ($\Delta n_{21}=n_2-n_1<0$, Figure 3.11c), respectively.

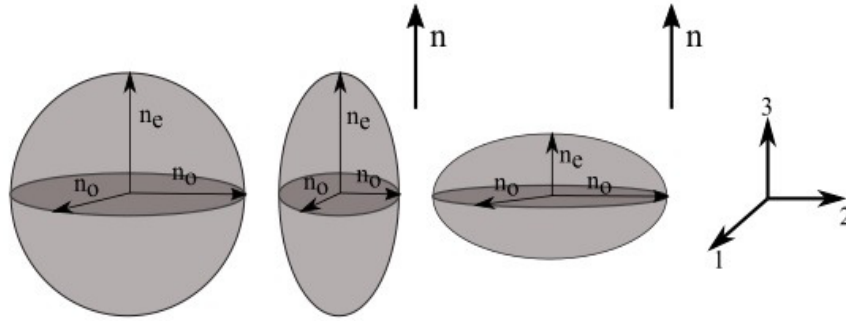


Figure 3.11 Indicatrices for (a) an isotropic, (b) uniaxial positive anisotropic and (c) uniaxial negative anisotropic materials (Wahlstrom, 1969; Stoiber, 1994; Simões, 2019).

In the case of uniaxial lyotropic nematic phases, there exists opposite situation with respect to the thermotropic counterparts. In the micelles of the lyotropic N_D phase, surfactants are packed in the micelles parallel to the optical axis of the phase, i.e. surfactant molecular long axis aligns in the direction of the optical axis, and the indicatrix indicates the positive birefringences, however, the surfactant molecular long axes are perpendicular to the optical axis of the N_C phase, which results in that the N_C phase has negative birefringence (Kazanci, 2003). Unlike lyotropic uniaxial nematic phases, the values of three refractive indices are not equal to each other in the N_B phases, $n_1 \neq n_2 \neq n_3$ (indeed, $n_1 \leq n_2 \leq n_3$) and the indicatrix is a completely asymmetric ellipsoid, giving either biaxial positive indicatrix or biaxial negative indicatrix (Figure 3.12). If the $n_3 - n_2 > n_2 - n_1$, the N_B phase is optically positive, N_B^+ (N_B^-), see Figure 3.12a (Figure 3.12b).

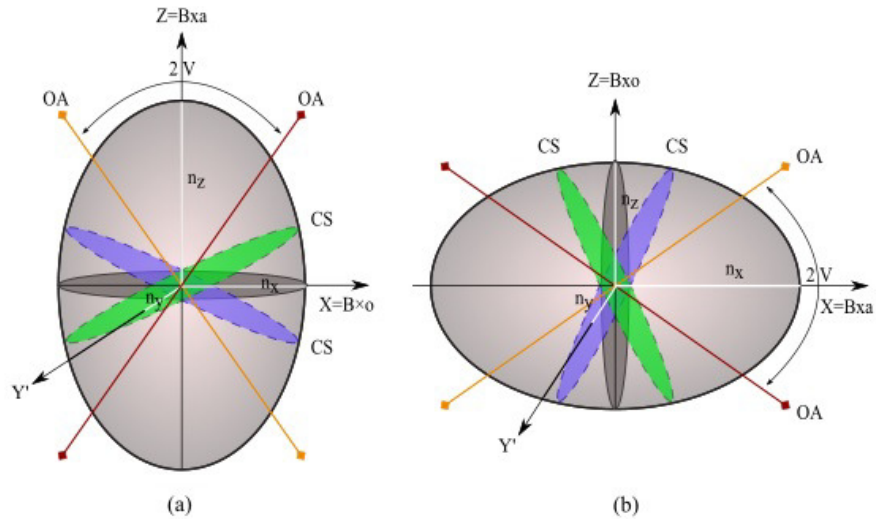


Figure 3.12 (a) Biaxial positive indicatrix, (b) Biaxial negative indicatrix. OA: optical axis; CS: circular section; Bxa: Acute bisectrix; Bxo: Obtuse bisectrix (Simões, 2019).

In 1983, Galerne and Marcerou proposed an alternative method, so-called laser conoscopy, to measure the birefringences of three lyotropic nematic phases precisely (Galerne, 1983). Indeed, this method assumes that the micelles have orthorhombic symmetry as predicted in the IBM model of the lyotropic nematic phases. The laboratory frame axes are chosen as shown in the Figure 3.13.

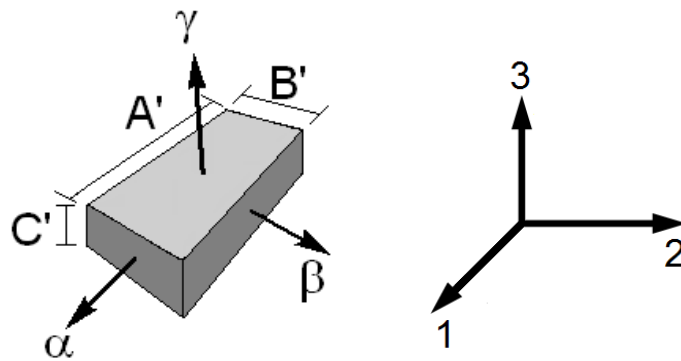


Figure 3.13 In the laser conoscopy techniques, it is assumed that micelles are thought to have orthorhombic symmetry in three nematic phases as proposed in the IBM model, given in the Figure 1.7 The laboratory frame axes were defined as follows: the horizontal plane was defined by the two orthogonal axes 1 and 2; the magnetic field was aligned along the axis 1; axis 3 was vertical and parallel to the laser beam propagation direction.

Simply, the laser conoscopy technique is carried out for the measurement of the optical birefringences of the nematic phases as a function of temperature. In this technique, the well-aligned sample is necessary. For this purpose, a small amount of water-based ferrofluid (Ferrotec) is added to each lyotropic mixture to obtain well-oriented nematic samples in a magnetic field.

After the ferrofluid is distributed in the mixtures well, some amount of the sample is put in the sample cell, which is made of two circular optical glasses (Helma) and a glass o-ring (Helma), providing a liquid crystalline film of 2.5 mm thick. Then, the sample cell is placed in a sample holder of the laser conoscopy set-up, see Figure 3.14 The temperature was controlled by a Lakeshore 335 model temperature controller (with Pt102 sensor and an accuracy of $\pm 0.001^\circ\text{C}$) and the heat distribution to all system was provided by a water circulating bath (Polyscience AD07R with an accuracy of $\pm 0.01^\circ\text{C}$).

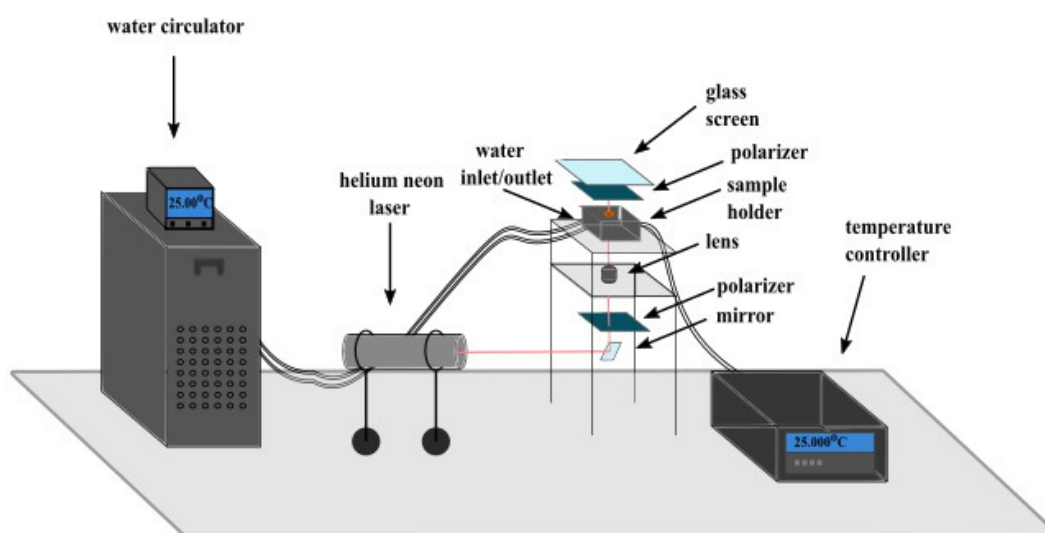


Figure 3.14 Schematic representation of laser conoscopy set-up.

Because the orientation of the local director of the micelles with respect to the optical axis of the nematic phases is a key point to obtain successful results for the temperature dependence of the birefringences measurements, an external magnetic field (~ 2.3 kG, checked with Lakeshore 475 Model Gaussmeter) was applied to the

samples. Remember that the orientation of three nematic phases are different from one another in the magnetic field.

The birefringence measurements were carried out starting from the well-aligned N_D phase. The alignment process is as follows, as described well in the Ref. (Akpınar and Neto, 2012a): the samples were kept at a fixed temperature for a period of time of about 30-60 min. Then, the temperature was varied step by step, depending on the proximity of the phase transition temperature, i.e. the nearer the transition temperature, the narrower the step. At each new temperature the sample was left at rest for at least 10 min for establishing the thermal equilibrium. From time to time, in the N_D (N_B) phase, the sample was turned of an angle of about $\pm\pi/2$ ($\pm\pi/6$) around axis 3 to improve the sample orientation.

The laser conoscopy furnishes the two main optical birefringences, $\Delta n = n_2 - n_1$ and $\delta n = n_3 - n_2$, which were measured as a function of temperature. The birefringences were obtained by measuring the refraction angles of the interference figures (isogyres or isochromates) in the plane perpendicular to the laser propagation direction (Born, 1980). While $\Delta n=0$ ($\Delta n \neq 0$) and $\delta n \neq 0$ ($\delta n = 0$) for the N_D (N_C) phase, $\Delta n \neq 0$ and $\delta n \neq 0$ for the N_B phase.

3.5 Polarizing Optical Microscopy

Another important device to examine nematic phases and transitions of lyotropic liquid crystals is polarizing optical microscope. All measurements were done by using Nikon Eclipse E200POL (Japan) microscope with water circulator and heat stabilizer as Polyscience SD07R with an accuracy of $\pm 0.04^\circ\text{C}$ and Linkam LTS120E with a temperature stability of, at least, 0.1°C respectively. In the measurement process, a 0,2mm slide was filled with homogeneous liquid crystalline sample and placed into system. To prevent water and sample loss from, both ends of the slide were sealed with polymer. Most significant benefit of this technique is it shows phases and transitions that laser conoscopy method can not achieve.

4. RESULT AND DISCUSSION

Table 4.1 shows the compositions of the lyotropic mixtures of tetradecylalkylammonium bromide (TAABr) at constant constituents' concentrations by changing the surfactant head groups and the observed mesophases. By this way, we studied the effect of the symmetric and asymmetric head-group growth on obtaining the biaxial nematic phases. As expected when the head group size of TAABr molecules grows by the addition of $-\text{CH}_2$ group, the surface charge density of the head groups at the micelle surfaces and the number of counterions bound to the micelle surfaces decrease (Akpinar et al., 2018b). Because the counterions not only screen the repulsions at the micelle surfaces but also affect the micelle surface curvature, the decrease in the counterion binding to the micelle surface may cause the stabilization of different lyotropic liquid crystalline structures. In this study, we observed the lyotropic lamellar (L_α), nematic (N), isotropic (I) and hexagonal (H_1) phases in the mixtures studied (Table 4.1). The textures of the lyotropic phases were confirmed by polarizing optical microscopy (Figure 4.1).

Table 4.1 Lyotropic mixture compositions in mole % and the observed phase types of the studied tetradecylalkylammonium bromides.

TAABr	X_{TAABr}	X_{NaBr}	X_{DeOH}	X_{water}	Phase type
TDMABr	3.93	0.30	0.94	94.83	L_α , I
TTMABr	3.93	0.30	0.94	94.83	N_C , N_B , N_D , I
TDMEABr	3.93	0.30	0.94	94.83	N_C , N_C+I , I
TDEMABr	3.93	0.30	0.94	94.83	N_C , N_C+H_1 , H_1 , H_1+I , I
TTEABr	3.93	0.30	0.94	94.83	H_1+I , I
TTPABr	3.93	0.30	0.94	94.83	I
TTBABr	3.93	0.30	0.94	94.83	Phase separation

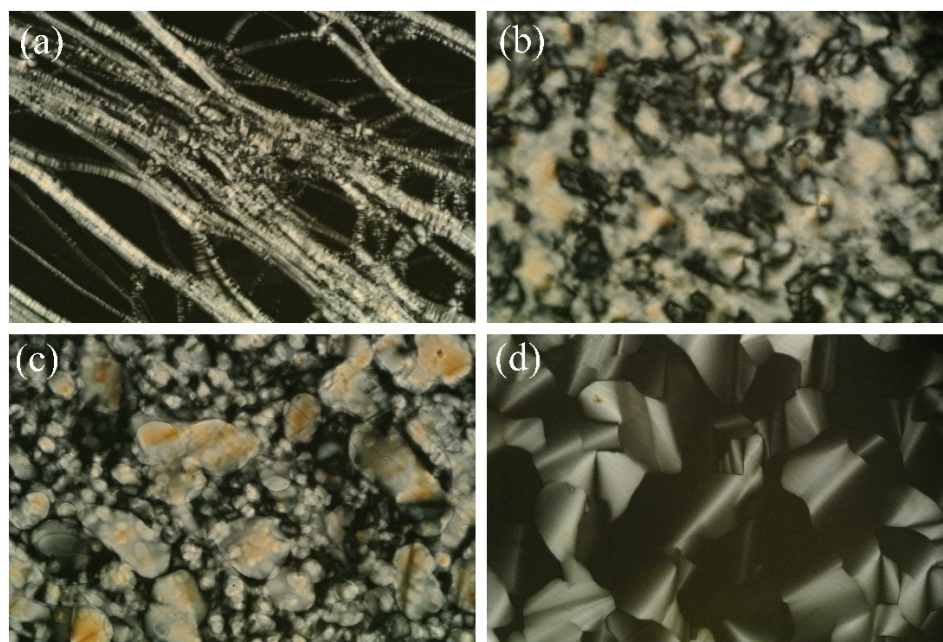


Figure 4.1 Textures of the tetradecylalkylammonium bromide surfactants observed by polarizing optical microscopy: (a) L_{α} for TDMABr at 35.0°C, (b) N_C for TDEMABr at 15.0°C, (c) N_C+H_1 for TDEMABr at 25.0°C and (d) H_1 for TDEMABr at 55.0°C. Magnification of objective: 10x and the sample thicknesses are 200 μm .

The surfactant molecules are packed mainly in the flattest part of the large molecular aggregates in the lamellar phase. In the case of the hexagonal phase, there exist long rod-like molecular aggregates, arranged in the hexagonal structure. If we compare both phases in terms of the molecular-aggregates surface curvature, in the lamellar (hexagonal) phases the aggregates have the lowest (highest) surface curvature (Blackmore and Tiddy, 1988). This indicates that the repulsions between the surfactant head groups at the aggregates' surfaces are at the minimum level in the lamellar phase, and at the maximum level in the hexagonal phase. Then, the area per surfactant head group at the aggregates' surface in the lamellar phase is expected to be smaller than that in the hexagonal phase. Blackmore and Tiddy (1988) reported the mesophase behavior of some dodecyl-, tetradecyl- and hexadecyltrialkylammonium bromide surfactants in water, where their ionic head groups were trimethyl-, triethyl-, and tripropylammonium. They prepared and investigated the surfactants/water binary mixtures to compare the relative effect of the head-group size on the mesophase structures by "penetration optical microscope technique". Their results are similar to those obtained in the present study, except

that we prepared quaternary mixtures of surfactant/NaBr/DeOH/water. Moreover, they did not observe any nematic region in their phase diagrams.

The birefringences (Δn and δn , for details about the technique and definitions of these birefringences see Galerne and Marcerou, 1983; Akpinar et al., 2012a) and the uniaxial-to-biaxial nematic phase transitions were determined by using the laser conoscopy. As discussed elsewhere (Galerne and Marcerou, 1983), in the case of the uniaxial nematic phases, there is only one non-zero birefringence, and in the biaxial phase both birefringences are different from zero. The results are given in Figure 4.2. Previous experimental studies indicated that the higher the birefringences the bigger the micelles (Akpinar et al., 2018a). There exist three nematic phases in the mixture with TTMABr (Figure 4.2a). Additional $-\text{CH}_2$ in the head group of the surfactant molecules causes, first, the destabilization of both N_D and N_B phases (Figure 4.2b) and then, the appearance of the H_1 phase in the biphasic region (Figure 4.2c). The laser conoscopy results are in good agreement with the textures observed under the polarizing optical microscope (Figure 4.1b, c and d). Specially, if we compare the birefringence values at 10.0°C , TTMABr, TDMEABr and TDEMABr have birefringences values of $\sim 2.3 \times 10^{-3}$, $\sim 2.0 \times 10^{-3}$ and $\sim 1.7 \times 10^{-3}$, respectively. This indicates that, as the head-group size increases, the micelle size get smaller.

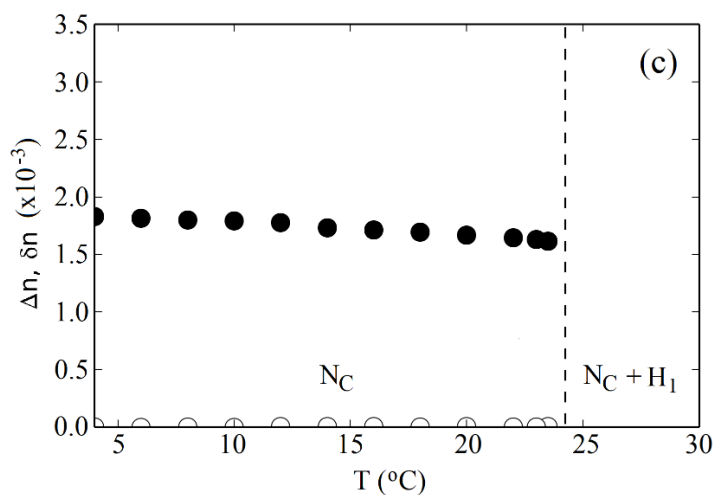
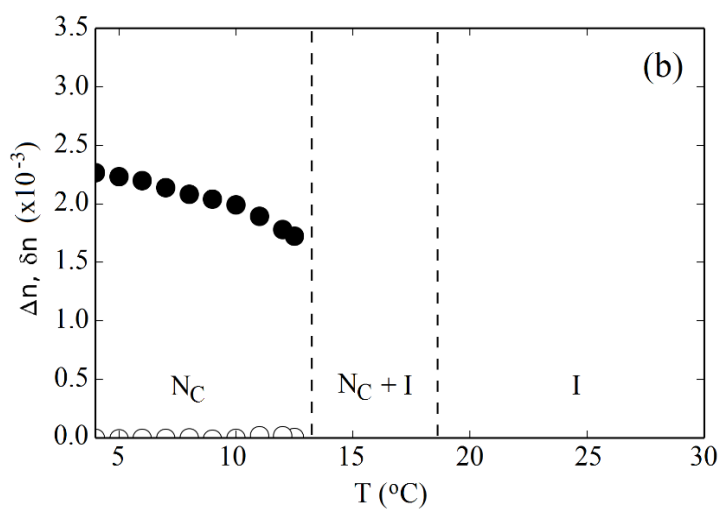
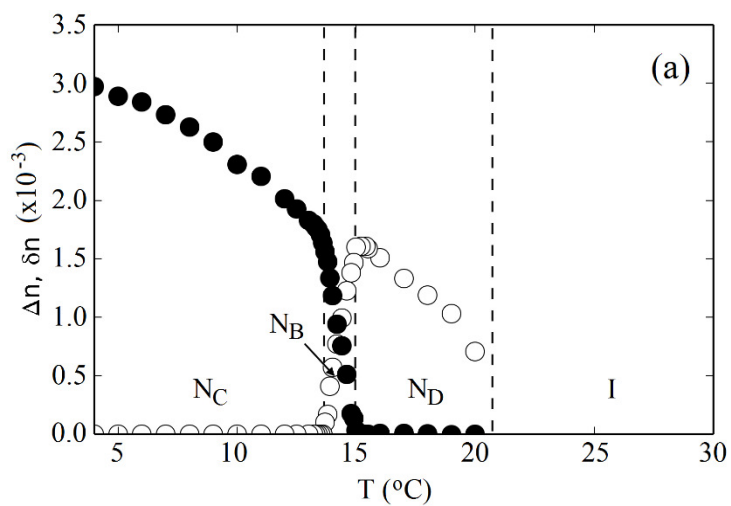


Figure 4.2 Temperature dependence of the birefringences, Δn (\bullet) and δn (\circ), for mixtures with (a) TTMABr, (b) TDMEABr, and (c) TDEMABr. N_D , N_B and N_C are the lyotropic discotic nematic, biaxial nematic and calamitic nematic phases, respectively. H_1 is the hexagonal phase. I represent the isotropic phase.

The authors of Ref. (Blackmore and Tiddy, 1988) and Refs. (Mitchel et al., 1983; Tiddy, 1985) stated that there is a relation between the surface area per head groups (a_s) of TAABr bromide surfactants and the stabilization of different lyotropic structures. For instance, if a_s is bigger than $\sim 70 \text{ \AA}^2$, hexagonal phase is most likely to be observed in the phase diagram. However, when the value of the a_s is smaller than $\sim 47 \text{ \AA}^2$, the hexagonal phase is not present in the phase diagram and just lamellar phase is stabilized. This is in good agreement with our results given in Table 4.1. From TDMABr to TTPABr, the surfactant head groups of TAABr molecules symmetrically and asymmetrically grow, i.e. their a_s values increase, and while the lamellar phase is not further observed, the nematic and hexagonal phases are stabilized.

In the present work, we focused our attention on the stabilization of the different lyotropic nematic phases and its relation with the parameter a_s . Before discussing its role, it is important to mention the mechanisms reported in the literature to explain the stabilization of the lyotropic nematic phases. In early studies, researchers assumed that the N_D and N_C phases consisted of disc-like (oblate ellipsoid) and cylindrical- or rod-like (prolate ellipsoid) micelles, respectively (Stroobants and Lekkerkerker, 1984; Rabin et al., 1982; Chen and Deutch, 1984). They also proposed that the N_B phase is not a thermodynamically stable phase, being a coexistence of the two uniaxial N_D and N_C phases. However, some other researchers argued from theoretical and strong experimental evidences that the N_B phase is a thermodynamically stable distinct phase. Among the mechanisms stated in the literature, a model, so-called ‘Intrinsically Biaxial Micelles, IBM’ model (Neto and Salinas, 2005; Neto et al., 1985), seems us to be the best model to explain the stabilization of the lyotropic nematic phases. According to the IBM model, the orthorhombic micelles with the dimensions A, B and C, where C corresponds to the micelle bilayer thickness, exist in all three nematic phases. Different orientational fluctuations are the driving mechanisms for the stabilization of the three nematic phases. Furthermore, the continuous change in micelle sizes along two-dimensions (both A and B) trigger the changes in the orientational fluctuations. Of course, the micelle surface curvatures in the N_D phases are a little different than those in the N_C ones. This is supported by our results given in Table 4.1. The TDMABr, which has the lowest a_s with respect to other studied surfactants, stabilizes the lamellar phase and, going from this surfactant to the TTEABr, the lamellar and N_D phases are

destabilized, and the N_C , hexagonal and I phases appear. It means that the micelle surface curvature in the N_D (N_C) phase is not exactly same but similar to the lamellar (hexagonal), considering the a_s values given in the literature. The micelle surface curvature (related to a_s) is expected to increase in the sequence of L_α , N_D , N_B , N_C , H_1 and I. Dawin et al. (2009) also reported the packing parameters (Π) of cesium perfluorooctanoate/ D_2O lyotropic mixture as a function of the temperature from nematic-isotropic to nematic-lamellar phase boundaries. According to their results, Π increases along the whole nematic phase region, towards the lamellar phase. Because Π is inversely proportional to a_s , $\Pi = V_{\text{hyd}} / (l_{\text{max}} a_s)$, where V_{hyd} and l_{max} are the volume of the hydrophobic chain and the maximum length of the hydrophobic chain of the surfactant, respectively, a_s decreases from the isotropic to the lamellar phase (Dawin et al., 2009). Thus, in our case, from the lamellar phase of TDMABr to the isotropic phase of TTEABr, passing through nematic and hexagonal phase region, V_{hyd} and l_{max} are constant for all TAABr molecules. The different packing of the surfactant molecules, stabilizing different lyotropic structures, arises from the symmetric and asymmetric head-group growth (indeed, the change in their a_s values) of the TAABr molecules.

Our results indicate that the area per surfactant head group at the micelle surface is an important parameter to obtain different nematic phases, especially the N_B phase. However, it would be interesting to know how: a) the a_s values and b) the degree of counterion binding at the micelle surfaces change with the head-group growth of the TAABr molecules. Some studies in the literature stated that, since lyotropic liquid crystals and the isotropic dilute micellar solutions consist of amphiphilic molecular aggregates, some parameters obtained from the latter one may be applicable to the former one. For instance, the addition of strong electrolytes to the mixtures gives rise to an increase in micelle dimensions in lyotropic mixtures and isotropic micellar solutions. Because of this, micellization parameters such as critical micelle concentrations (cmc) and the degree of counterion binding to the micelles, β , of tetradecylalkylammonium bromides and micellization Gibbs energies as a function of symmetric and asymmetric head-group growth at 30.0°C were measured with electrical conductimetry technique. The cmcs of the surfactants correspond to the abrupt break point observed on the specific conductivity versus total surfactant

concentration curve (Figure 4.3). Thus, two linear curves are obtained below and above the cmc, and the ratio of the slope of the latter curve to the former one gives the ionization degree of the counterion, α , which is related to β as $\alpha=1-\beta$. The micellization Gibbs free energies, $\Delta_{mic}G$, of the surfactants were evaluated by the equation, $\Delta_{mic}G = (1 + \beta)RT \ln X_{cmc}$, (Moulik et al., 1996; Velego et al., 2000), where R is the ideal gas constant ($8.3145 \text{ J.K}^{-1}.\text{mol}^{-1}$), X_{cmc} is the mole fraction of the surfactant at the cmc in the absence of electrolyte (or salt), and T is the absolute temperature. The micellization Gibbs free energies are given in Table 4.2. Our values of the cmc, β and $\Delta_{mic}G$ for tetradecyltrimethylammonium bromide at 30.0°C are, within the experimental error, in good agreement with those from the literature (Buckingham et al., 1982; Maiti et al., 2009; Zana, 1980). The change of cmc with an increase in the number of carbon atoms in the head groups, i.e. the head-groups growth, indicates that the cmc decreases slightly (strongly) from TTMABr to TTEABr (from TTEABr to TTBABr), Figure 4.3-4.9 and Table 4.2. In other words, the micellization becomes more favorable as the head groups of the surfactants grow symmetrically and asymmetrically. However, TDMABr, where two methyl and one hydrogen are bound to the central nitrogen atom in its head group, has lower cmc than TTMABr. In general, the decrease (increase) in the cmc is the indicative of the increase (reduction) in the degree of counterion binding (dissociation) to the micelles, which favors the micellization. But, in the case of tetradecylalkylammonium bromides, the decrease in their cmc values as a function of the head-group size, by the addition of $-\text{CH}_2$ group in their head groups, is a consequence of the increase in the hydrophobic character of the head groups. At the same time, while the dehydration of the head groups at the micelle surfaces occurs, the hydrophobic interactions between the neighboring head groups promote the micelle formation. Thus, less amount of counterions are bound to the micelle surfaces, i.e. the degree of counterion binding decreases although their cmcs decrease, as the head group of the tetradecylalkylammonium bromides grow.

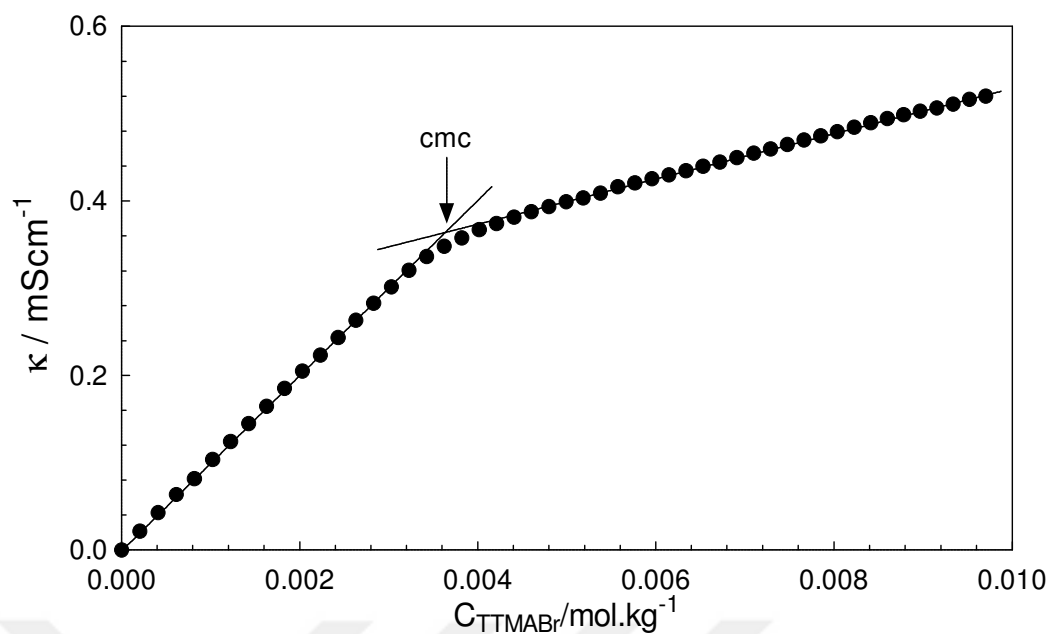


Figure 4.3 Specific conductivity versus total TTMABr concentration at $30.0\pm 0.1^\circ\text{C}$. For other TAABr surfactants, similar results were obtained. Solid lines are linear fits to the experimental points.

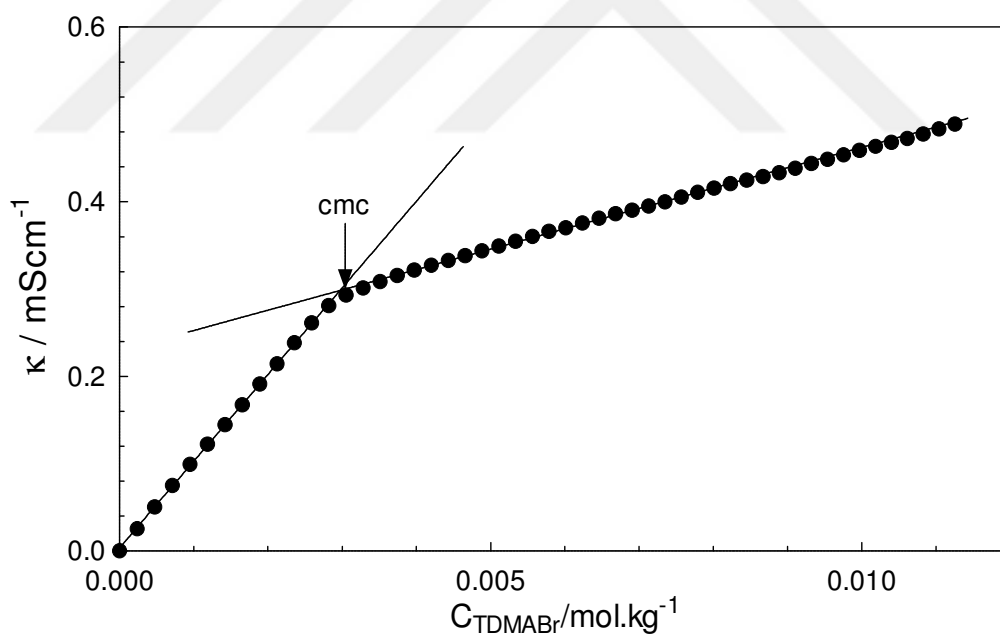


Figure 4.4 Specific conductivity versus total TDMABr concentration at $30.0\pm 0.1^\circ\text{C}$.

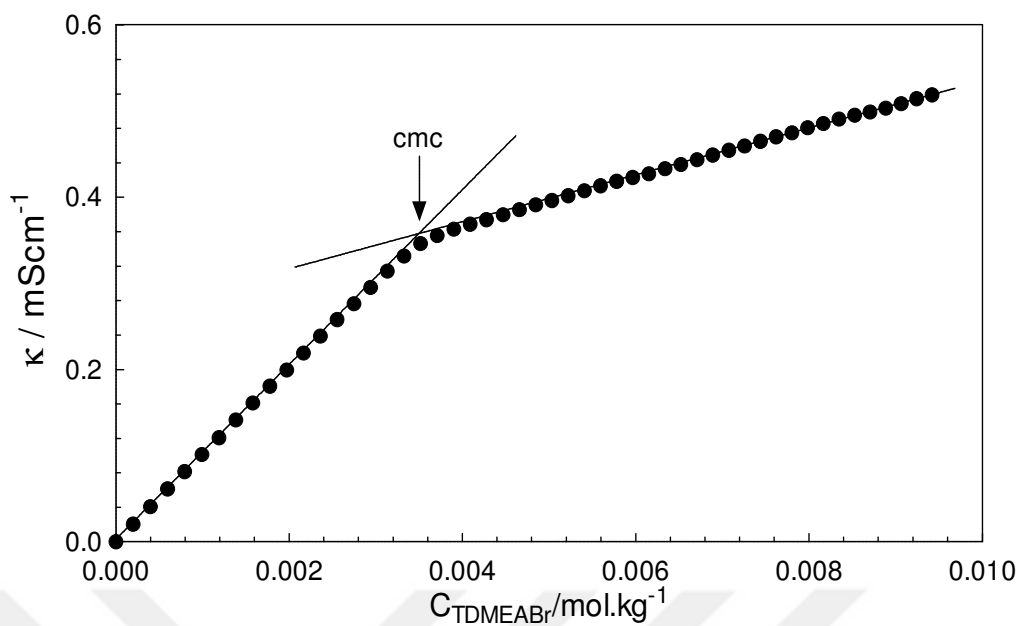


Figure 4.5 Specific conductivity versus total TDMEABr concentration at $30.0 \pm 0.1^\circ\text{C}$.

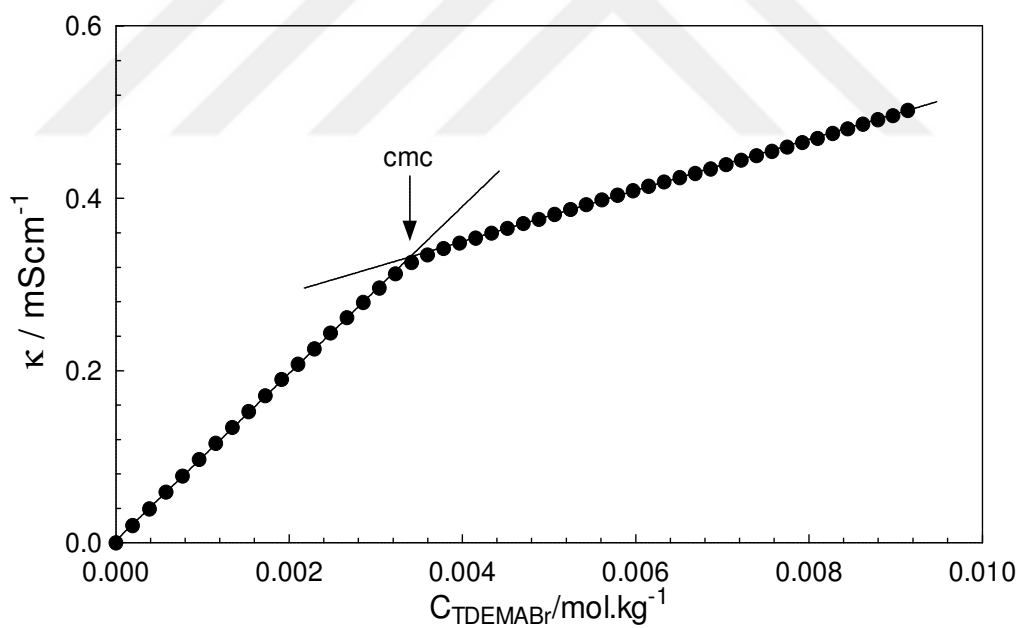


Figure 4.6 Specific conductivity versus total TDEMABr concentration at $30.0 \pm 0.1^\circ\text{C}$.

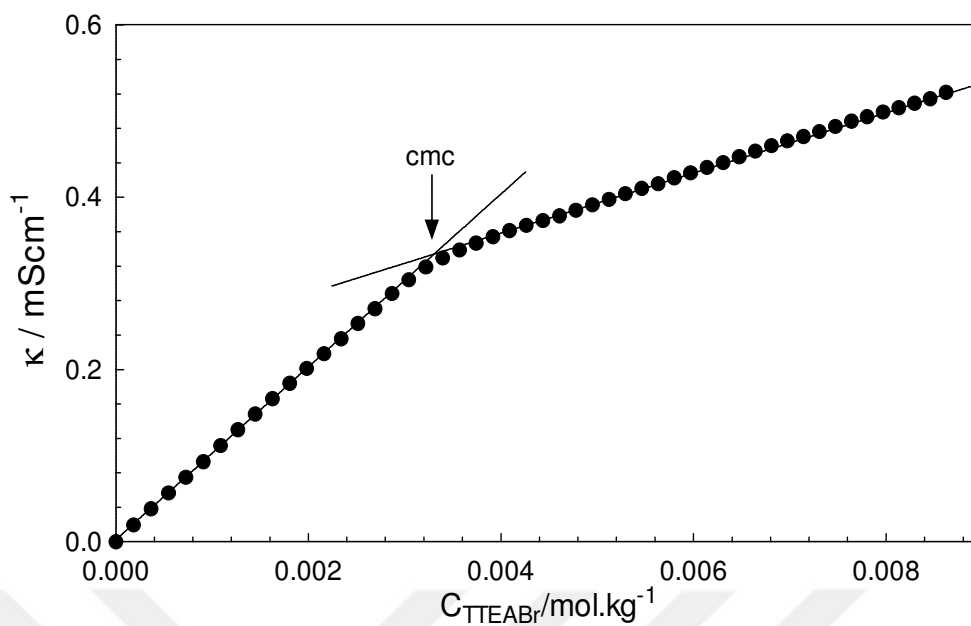


Figure 4.7 Specific conductivity versus total TTEABr concentration at $30.0 \pm 0.1^\circ\text{C}$.

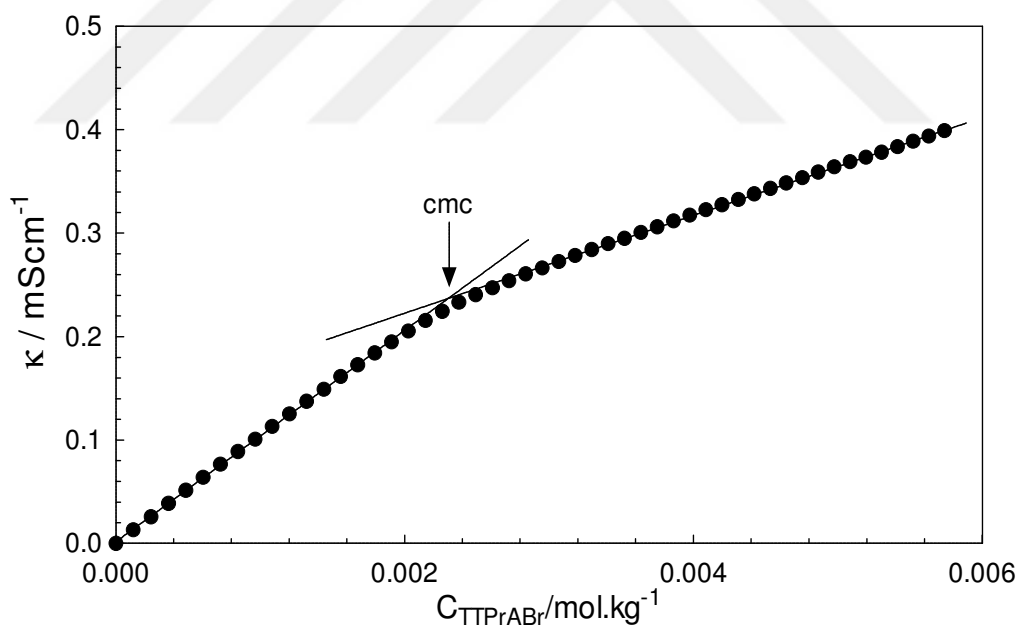


Figure 4.8 Specific conductivity versus total TTPrABr concentration at $30.0 \pm 0.1^\circ\text{C}$.

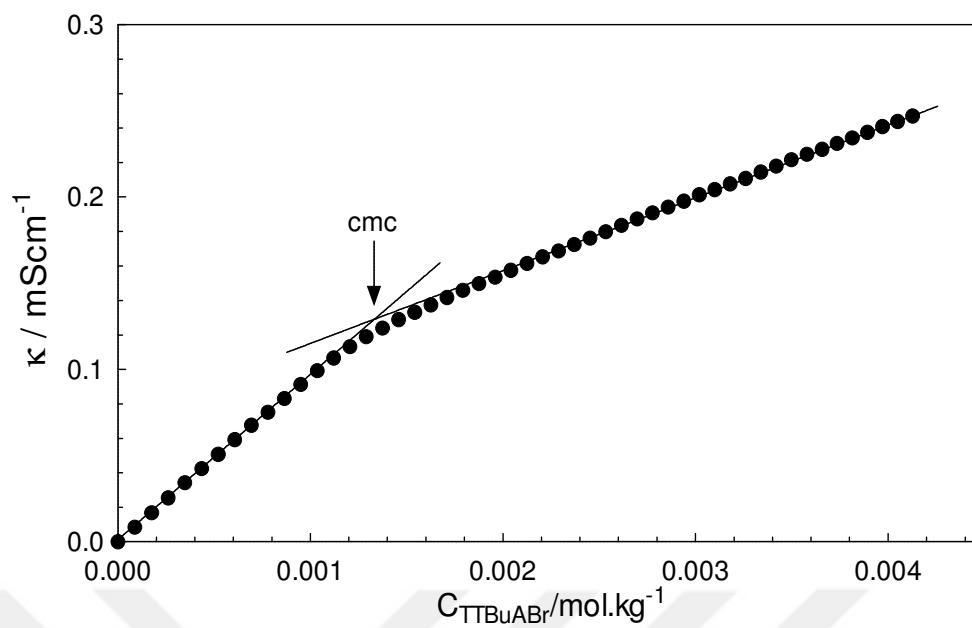


Figure 4.9 Specific conductivity versus total TTBuABr concentration at $30.0 \pm 0.1^\circ\text{C}$.

Table 4.2 Critical micelle concentrations (cmc) of tetradecylalkylammonium bromide surfactants at 30°C. The numbers between parentheses are from literature.

Surfactant	cmc/mmolkg ⁻¹	β	$\Delta_{mic}G/kJ.mol^{-1}$	$a_s / \text{\AA}^2$
TDMABr	2.97±0.04	0.772±0.002	-43.94±0.11	-----
TTMABr	3.64±0.05 (3.61 ^a , 3.78 ^b , 3.84 ^c , 3.67 ^d)	0.740±0.003 (0.74 ^c , 0.73 ^f , 0.76 ^c , 0.77 ^a , 0.68 ^d)	-42.24±0.12 (-42.5 ^c , -41.3 ^g , -40.62 ^d , -42.9 ^a)	(87 ^h , 75.3 ^j)
TDMEABr	3.50±0.02	0.721±0.002	-41.96±0.08	-----
TDEMABr	3.39±0.02	0.697±0.002	-41.51±0.06	-----
TTEABr	3.28±0.01	0.647±0.002 (0.65 ^e)	-40.40±0.03	(90 ^g , 78.4 ^b)
TTPrABr	2.29±0.04	0.546±0.004 (0.54 ^e)	-39.32±0.10	(93 ^g , 81.4 ^b)
TTBuABr	1.32±0.01	0.542±0.005 (0.54 ^e)	-41.37±0.17	(97 ^g , 84.7 ^b)

From the references: ^a [35], ^b [36], ^c [37], ^d [38], ^e [22], ^f [39], ^g [40], ^h [41], ^j [42].

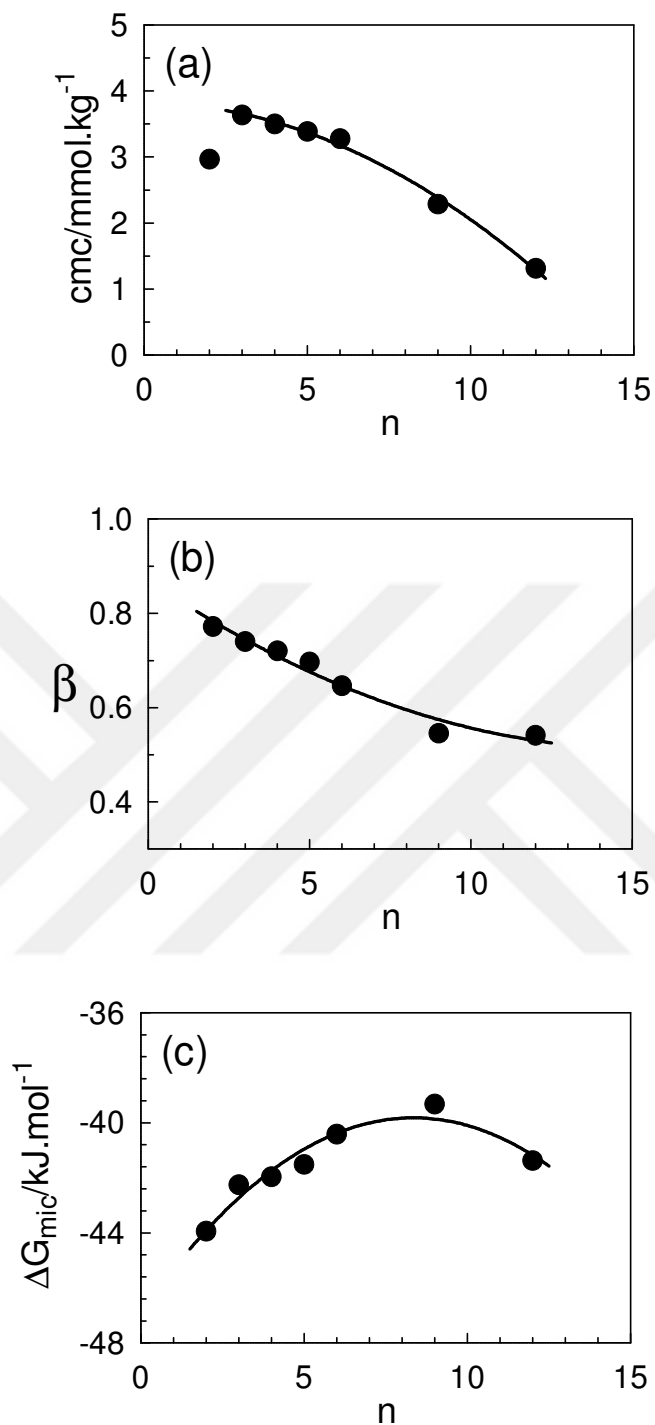


Figure 4.10 (a) Critical micelle concentrations, (b) degree of counterion bindings and (c) micellization Gibbs free energies of TAABr surfactants. n is the number of carbon atoms in the headgroups of the surfactants, where $n=2, 3, 4, 5, 6, 9$ and 12 correspond to TDMABr, TTMABr, TDMEABr, TDEMABr, TTEABr, TTPrABr and TTBuABr, respectively.

The behavior of the micellization Gibbs free energies with the number of carbon atoms in the headgroups of the surfactants, n , is in good agreement with the literature (Buckingham et al., 1993; Rodriguez et al., 2007). The value of the $\Delta_{\text{mic}}G$ of TTBABr is very similar to that of TDEMABr and this may be attributed to the penetration of some alkyl groups in the head group of the former one towards the deeper of the micelle surfaces.

If the results of the isotropic micellar solutions of the tetradecylalkylammonium bromide surfactants are compared to their lyotropic liquid crystal results, the a_s value of the surfactants seems to be a new control parameter to obtain different lyotropic phases, especially the N_B one.



5. CONCLUSIONS

In this study, we aimed to investigate the effect of the growth of the surfactant head groups on stabilizing the different nematic phases and the uniaxial-to-biaxial phase transitions. To do so, we studied isotropic micellar solutions and lyotropic liquid crystalline mixtures of tetradecylalkylammonium bromide surfactants. The laser conoscopy and polarizing optical microscopy results of the lyotropic nematic phases showed that the surfactant head-group size is one important parameter to obtain different lyotropic nematic phases. This parameter, the minimum area per surfactant head group (a_s), has to be considered choosing the suitable surfactant molecules to prepare a lyotropic mixture giving the N_B phase. The greater the head group size (i.e. the a_s) causes the observation of the N_C phase or hexagonal phase, the smaller the head group size results in the formation of three nematic phases or lamellar phase. Furthermore, the uniaxial-to-biaxial phase transition is of second order as predicted by the Landau type mean-field theory.

6. REFERENCES

- Acharya BR, Primak A and Kumar S (2004) "Biaxial Nematic Phase in Bent-Core Thermotropic Mesogens", *Phys Rev Lett*, 92: 145506.
- Akpinar E, Canioz C, Turkmen M, Reis D and Neto AMF (2018a) "Effect of the Surfactant Alkyl Chain Length on the Stabilization of Lyotropic Nematic Phases", *Liq Cryst*, 45(2): 219-229.
- Akpinar E, Otluglu K, Turkmen M, Canioz C, Reis D and Neto AMF (2016a) "Effect of the Presence of Strong and Weak Electrolytes on the Existence of Uniaxial and Biaxial Nematic Phases in Lyotropic Mixtures", *Liq Cryst*, 43: 1693-1708.
- Akpinar E, Reis D and Neto AMF (2012a) "Lyotropic Mixture Made of Potassium Laurate/1-Undecanol/K₂SO₄/Water Presenting High Birefringences and Large Biaxial Nematic Phase Domain: A Laser Conoscopy Study", *Eur Phys J E: Soft Matter and Biological Physics*, 35(50): 1-9.
- Akpinar E, Reis D and Neto AMF (2012b) "Effect of Alkyl Chain Length of Alcohols on Nematic Uniaxial-to-Biaxial Phase Transitions in a Potassium Laurate/Alcohol/K₂SO₄/Water Lyotropic Mixture", *Liq Cryst*, 39(7): 881-888.
- Akpinar E, Reis D and Neto AMF (2015) "Effect of Hofmeister Anions on the Existence of the Biaxial Nematic Phase in Lyotropic Mixtures of Dodecyltrimethylammonium Bromide/Sodium Salt/1-Dodecanol/Water", *Liq Cryst*, 42(7): 973-981.
- Akpinar E, Turkmen M, Canioz C and Neto AMF (2016b) "Role of Kosmotrope-Chaotrope Interactions at Micelle Surfaces on the Stabilization of Lyotropic Nematic Phases", *Eur Phys J E*, 39: 107.
- Akpinar E, Yurdakul S and Neto AMF (2018b) "Comparison Between Lyotropic Cholesteric Phase Behavior with Partly Fluorinated Surfactants and Their Exact Hydrogenated Counterparts", *J Mol Liq*, 259: 239-248.
- Alben R (1973) "Phase Transitions in a Fluid of Biaxial Particals", *Phys Rev Lett*, 30(17): 778-781.
- Amaral LQ and Tavares MR (1980) "On the Possible Formation of Macromicelles in a Lyomesophase", *Mol Cryst Liq Cryst Lett*, 56: 203-208.
- Amaral LQ, Pimentel CA, Tavares MR and Vanin JA (1979) "Study of a Magnetically Oriented Lyotropic Mesophase", *J Chem Phys*, 71(7): 2940-2945
- Aniansson, EAG, Wall SN, Almgren M, Hoffmann H, Kielmann I, Ulbricht W, Zana R, Lang J and Tondre C (1976) "Theory of the Kinetics of Micellar Equilibria and Quantitative Interpretation of Chemical Relaxation Studies of Micellar Solutions of Ionic Surfactants", *J Phys Chem*, 80: 905-922.

- Bartolino R, Chiaranza T, Meuti M and Compagnoni R (1982) “Uniaxial And Biaxial Lyotropic Nematic Liquid Crystals”, *Phys Rev A*, 26(2): 1116-1119.
- Berardi R, Muccioli L, Orlandi S, Ricci M and Zannoni C (2008) “Computer Simulations of Biaxial Nematics”, *J Phys: Condens Matter*, 20: 463101.
- Biscarini F, Chiccoli C, Pasini P, Semeria F and Zannoni C (1995) “Phase Diagram and Orientational Order in a Biaxial Lattice Model: A Monte Carlo Study”, *Phys Rev Lett*, 75: 1803– 1806.
- Blackmore ES and Tiddy GJT (1988) “Phase Behaviour and Lyotropic Liquid Crystals in Cationic Surfactant-Water Systems”, *J Chem Soc Faraday Trans 2*, 84(8): 1115-1127.
- Braga WS, Santos OR, Luders DD, Kimura NM, Sampaio AR, Simões M and Palangana AJ (2016) “Refractive Index Measurements in Uniaxial and Biaxial Lyotropic Nematic Phases”, *J Mol Liq*, 213: 186-190.
- Buckingham SA, Garvey CJ and Warr GG (1993) “Effect of Head-Group Size on Micellization and Phase Behavior in Quaternary Ammonium Surfactant Systems”, *J Phys Chem*, 97: 10236-10244.
- Camp PJ and Allen MP (1997) “Phase Diagram of the Hard Biaxial Ellipsoid Fluid”, *J Chem Phys*, 106: 6681.
- Charvolin J, Levelut AM and Samulski ET (1979) “Lyotropic Nematics: Molecular Aggregation and Susceptibilities”, *J Physique*, 40: 587-592.
- Chen ZY and Deutch JM (1984) “Biaxial Nematic Phase, Multiphase Critical Point, and Reentry Transition in Binary Liquid Crystal Mixtures”, *J Chem Phys*, 80: 2151-2162.
- Dawin UC, Lagerwall JPF and Giesselmann F (2009) “Electrolyte Effects on the Stability of Nematic and Lamellar Lyotropic Liquid Crystal Phases: Colligative and Ion-Specific Aspects”, *J Phys Chem B*, 113: 11414-11420.
- Dingemans TJ, Madsen LA, Zafiroopoulos NA, Lin W and Samulski ET (2006) “Uniaxial and Biaxial Nematic Liquid Crystals”, *Philos T R Soc A*, 364(1847): 2681-2696.
- Engels T and Rybinski W (1998) “Liquid Crystalline Surfactant Phases in Chemical Applications”, *J Mater Chem*, 8(6): 1313-1320.
- Filho AM, Laverde A and Fujiwara FY (2003) “Observation of Two Biaxial Nematic Mesophases in the Tetradecyltrimethylammonium Bromide/Decanol/Water System”, *Langmuir*, 19: 1127-1132.
- Freiser MJ (1970) “Ordered States of a Nematic Liquid”, *Phys Rev Lett*, 24: 1041-1043.
- Freiser MJ (1971) “Successive Transitions in a Nematic Liquid”, *Mol Cryst Liq Cryst*, 14: 165–182.

- Galerne Y (2006) "Comment on "Thermotropic Biaxial Nematic Liquid Crystals", Phys Rev Lett, 96(21): 219803.
- Galerne Y and Liébert L (1985) "Zigzag Disclinations in Biaxial Nematic Liquid Crystals", Phys Rev Lett, 55(22): 2449-2451.
- Galerne Y and Marcerou JP (1983) "Temperature Behavior of the Order-Parameter Invariants in the Uniaxial and Biaxial Nematic Phases of a Lyotropic Liquid Crystal", Phys Rev Lett, 51: 2109-2111.
- Galerne Y, Neto AMF and Liebert L (1987) "Microscopic Structure of the Uniaxial and Biaxial Lyotropic Nematics", J Chem Phys, 87: 1851–1856.
- Galindo A, Haslam AJ, Varga S, Jackson G, Vanakaras AG, Photinos DJ and Dunmur DA (2003) "The Phase Behavior of a Binary Mixture of Rodlike and Disklike Mesogens: Monte Carlo Simulation, Theory, and Experiment", J Chem Phys, 119(10): 5216-5225.
- Hashim R, Luckhurst GR and Romano S (1984) "Computer Simulation Studies of Anisotropic Systems", Mol Phys, 53: 1535.
- Hashim R, Luckhurst GR, Prata F and Romano S (1993) "Computer Simulation Studies of Anisotropic Systems. XXII. An Equimolar Mixture of Rods and Discs: A Biaxial Nematic?", Liq Cryst, 15(3): 283-309.
- Hendriks Y, Charvolin J and Rawiso M (1986) "Uniaxial-Biaxial Phase Transition in Lyotropic Nematic Solutions: Local Biaxiality in the Uniaxial Phase", Phys Rev B Condens Matter 33(5): 3534–3537.
- Henriques EF and Henriques VB (1997) "Biaxial Phases in Polydisperse Mean-Field Model Solution of Uniaxial Micelles", J Chem Phys, 107: 8036-8040.
- Ho CC, Hoetz RJ and El-Aasser MS (1991) "A Biaxial Lyotropic Nematic Phase in Dilute Solutions of Sodium Lauryl Sulfate-1-Hexadecanol-Water", Langmuir, 7: 630-635.
- Israelachvili JN (1991) Intermolecular and Surface Forces, First Edition, Academic Press, New York.
- Kazanci N, Nesrullajev A (2003) "Refracting and Birefringent Properties of Lyotropic Nematic Mesophases", Mater Res Bull, 38: 1003-1012.
- Kooij FM and Lekkerkerker H (2000a) "Liquid-Crystal Phases Formed in Mixed Suspensions of Rod- and Plate-like Colloids", Langmuir, 16: 10144-10149.
- Kooij FM and Lekkerkerker HNW (2000b) "Liquid-Crystalline Phase Behavior of a Colloidal Rod-Plate Mixture", Phys Rev Lett, 84: 781.
- Kooij FM and Lekkerkerker HNW (2001a) "Liquid-Crystal Phase Transitions in Suspensions of Plate-Like Particles", Philos T R Soc B, 359(1782): 985-995.
- Kooij FM, Beek D and Lekkerkerker HNW (2001b) "Isotropic–Nematic Phase Separation in Suspensions of Polydisperse Colloidal Platelets", J Phys Chem B, 105(9): 1696.

- Kooij FM, Vogel M and Lekkerkerker HNW (2000c) “Phase Behavior of a Mixture of Platelike Colloids and Nonadsorbing Polymer”, *Phys Rev E*, 62: 5397.
- Lagerwall JPF and Scalia G (2012). “A New Era for Liquid Crystal Research: Applications of Liquid Crystals in Soft Matter Nano-, Bio- and Microtechnology”, *Curr Appl Phys*, 12: 1387–1412.
- Lawson KD and Flautt TJ (1967) “Magnetically Oriented Lyotropic Liquid Crystalline Phases”, *J Am Chem Soc*, 89: 5489.
- Liu J, Guan R, Dong X, Dong Y (2018) “Molecular Properties of a Bent-Core Nematic Liquid Crystal A131 by Multi-Level Theory Simulations” *Mol Simulat*, 44(18): 1539-1543.
- Luckhurst GR (2001) “Biaxial Nematic Liquid Crystals: Fact or Fiction?”, *Thin Solid Films*, 393: 40–52.
- Luckhurst GR (2004) “Liquid Crystals – A Missing Phase Found At Last?”, *Nature*, 430: 413–414.
- Madsen LA, Dingemans TJ, Nakata M and Samulski ET (2004) “Thermotropic Biaxial Nematic Liquid Crystals”, *Phys Rev Lett*, 92: 145505.
- Madsen, LA, Dingemans TJ, Nakata M and Samulski ET (2006) “A Reply to the Comment by Yves Galerne”, *Phys Rev Lett* 96: 219804.
- Maiti K, Mitra D, Guha S and Moulik SP (2009) “Salt Effect on Self-Aggregation of Sodium Dodecylsulfate and Tetradecyltrimethylammonium Bromide: Physical Correlation and Assessment in the Light of Hofmeister (Lyotropic) Effect”, *J Mol Liquids*, 146: 44-51.
- Martínez-Ratón Y and Cuesta JA (2002) “Enhancement by Polydispersity of the Biaxial Nematic Phase in a Mixture of Hard Rods and Plates”, *Phys Rev Lett*, 89: 185701.
- Martínez-Ratón Y, Gonzalez-Pinto M and Velasco E (2016) “Biaxial Nematic Phase Stability and Demixing Behaviour in Monolayers of Rod-Plate Mixtures”, *Phys Chem Chem Phys*, 18: 24569.
- Melnik G and Saupe A (1987) “Microscopic Textures of Micellar Cholesteric Liquid Crystals”, *Mol Cryst Liq Cryst*, 145: 95-110.
- Mitchell DJ, Tiddy GJT, Waring L, Bostock T and McDonald MP (1983) “Phase Behaviour of Polyoxyethylene Surfactants with Water. Mesophase Structures and Partial Miscibility (Cloud Points)”, *J Chem Soc Faraday Trans*, 79: 975-1000.
- Moulik SP, Haque ME, Jana PK and Das AK (1996) “Micellar Properties of Cationic Surfactants in Pure and Mixed States”, *J Phys Chem*, 100: 701-708.
- Muhoray PP, Bruyn JR and Dunmur DA (1985) “Phase Behavior of Binary Nematic Liquid Crystal Mixtures”, *J Chem Phys*, 82: 5294-5295.

- Nasrin L, Kabir E and Rahman (2016) “External Magnetic Field-Dependent Tricritical Points of Uniaxial-To-Biaxial Nematic Transition”, *Phase Transit*, 89(2): 193-201.
- Nesmerak K and Nemcova I (2006) “Determination of Critical Micelle Concentration by Electrochemical Means”, *Anal Lett*, 39: 1023.
- Neto AMF and Amaral LQ (1980) “Study of Type I Lyomesophases by X-Ray Diffraction”, *Mol Cryst Liq Cryst*, 74(1-4): 109-119.
- Neto AMF and Galerne Y (2015) *Lyotropic Systems* in Luckhurst GR (ed) and Sluckin TJ (ed) *Biaxial Nematic Liquid Crystals, Theory, Simulation, and Experiment*, First Edition, pp. 285–304. Wiley, United Kingdom.
- Neto AMF, Galerne Y, Levelut AM and Liebert L (1985b) “Pseudo-Lamellar Ordering in Uniaxial and Biaxial Lyotropic Nematics-A Synchrotron X-Ray Diffraction Experiment”, *J Phys Lett*, 46(11): 409-505.
- Neto AMF, Liebet L and Galerne Y (1985a) “Temperature and Concentration Range of the Biaxial Nematic Lyomesophase in the Mixture Potassium Laurate/1-Decanol/D₂O”, *J Phys Chem*, 89: 3737-3739.
- Neto AMF, Salinas SRA (2005) *The Physics of Lyotropic Liquid Crystals: Phase Transitions and Structural Properties*, First Edition, Oxford University Press, New York.
- Oliveira EA, Liebert L and Neto AMF (1989) “A New Soap/Detergent/Water Lyotropic Liquid Crystal with a Biaxial Nematic Phase”, *Liq Cryst*, 5: 1669-1675.
- Pratibha R and Madhusudana NV (1985) “Evidence for two Coexisting Nematic Phases in Mixtures of Rod-Like and Disc-Like Nematogens”, *Mol Cryst Liq Cryst*, 1(3-4): 111-116.
- Pratibha R and Madhusudana NV (1990) “On the Occurrence of Point and Ring Defects in the Nematic-Nematic Coexistence Range of a Binary Mixture of Rod-like and Disc-like Mesogens, *Molecular Crystals and Liquid Crystals Incorporating Nonlinear Optics*”, *Mol Cryst Liq Cryst*, 178: 167-178.
- Quist PO (1995) “First Order Transitions to a Lyotropic Biaxial Nematic”, *Liquid Crystals*, 18: 623-629.
- Rabin Y, McMullen WE and Gelbart WM (1982) “Phase Diagram Behaviors for Rod/Plate Liquid Crystal Mixtures”, *Mol Cryst Liq Cryst*, 89: 67-76.
- Radley K and Saupe A (1978) “The Structure of Lyotropic Nematic Decylammoniumchloride and Bromide Systems by PMR of Monomethyltin Complexes and by Microscopic Studies”, *Mol Cryst Liq Cryst*, 44: 227-235.
- Radley K and Reeves LW (1976) “Effect of Counterion Substitution on the Type and Nature of Nematic Lyotropic Phases From Nuclear Magnetic Resonance Studies”, *J Phys Chem*, 80(2): 174-182.

- Reinitzer F (1888) “Beiträge zur Kenntniss des Cholesterins”, *Monatsh Chem*, 9: 421–441. (Translation to English in *Liq Cryst* 1989; 5: 7-18).
- Rodriguez MA, Munoz M, Graciani MM, Pachon MSD and Moya ML (2007) “Effects of Head Group Size on Micellization of Cetyltrialkylammonium Bromide Surfactants in Water-Ethylene Glycol Mixtures”, *Coll Surf A: Physicochem Eng Aspects*, 298: 177-185.
- Santos MBL, Galerne Y and Durand G (1984) “Critical Slowing Down of Biaxiality Fluctuations at the Uniaxial-to-Biaxial Phase Transition in a Lyotropic Disklike Nematic Liquid Crystal”, *Phys Rev Lett*, 53(8): 787-790.
- Sauerwein RA and Oliveira MJ (2016) “Lattice Model for Biaxial and Uniaxial Liquid Crystals”, *J Chem Phys* 144: 194904.
- Severing K and Saalwaachter K (2007) *Phase Biaxiality in Nematic Liquid Crystals in: A Thermotropic Liquid Crystals: Recent Advances*, pp 141-170, Springer, Netherlands.
- Sharma SR, Muhoray PP, Bergersen B and Dunmur DA (1985) “Stability of a Biaxial Phase in a Binary Mixture of Nematic Liquid Crystals”, *Phys Rev A*, 32(6): 3752.
- Shinoda K, Nakagawa T, Tamamushi B-I and Isemuta T (1963) *Colloidal Surfactants, Some Physicochemical Properties*, First edition, Academic Press, London.
- Simões M, Bertolino WHP, Tovar D, Braga W, Santos O, Luders DD, Sampaio AR and Kimura NM (2019) “Optical Signal and Optical Axes in Uniaxial and Biaxial Nematic Phases”, *Phase Transit*, DOI:10.1080/01411594.2018.1556269.
- Stoiber RE and Morse SA (1994) *Crystal Identification with the Polarizing Microscope*, First Edition, Chapman and Hall, New York
- Straley JP (1974) “Ordered Phases of a Liquid of Biaxial Particles”, *Phys Rev A*, 10: 1881-1887.
- Stroobants A and Lekkerkerker HNW (1984) “Liquid Crystal Phase Transitions in a Solution of Rodlike and Disklike Particles”, *J Phys Chem*, 88: 3669-3674.
- Taylor MP and Herzfeld J (1991) “Nematic and Smectic Order in a Fluid of Biaxial Hard Particles”, *Phys Rev A*, 44(6): 3742-3751.
- Taylor TR, Ferguson JL and Arora SL (1970) “Biaxial Liquid Crystals”, *Phys Rev Lett*, 24(8): 362.
- Tiddy GJT (1985) in: Eicke HF (ed) *Modern Trends of Colloid Science in Chemistry and Biology*, Birkhauser Verlag, Basel, p. 148.
- van den Pol E, Petukhov AV, Thies-Weesie DM, Byelov DV and Vroege GJ (2009) “Experimental Realization of Biaxial Liquid Crystal Phases in Colloidal Dispersions Of Boardlike Particles”, *Phys Rev Lett*, 103: 258301.

- Vanakaras AG and Photinos DJ (1997) "Theory of Biaxial Nematic Ordering in Rod-Disc Mixtures Revisited", *Mol Cryst Liq Cryst*, 299(1): 65-71.
- Vanakaras AG, Bates MA and Photinos DJ (2003) "Theory and Simulation of Biaxial Nematic and Orthogonal Smectic Phases Formed by Mixtures of Boardlike Molecules", *Phys Chem Chem Phys*, 5: 3700-3706.
- Vanakaras AG, McGrother SC, Jackson G and Photinos DJ (1998) "Hydrogen-Bonding and Phase Biaxiality in Nematic Rod-Plate Mixtures", *Mol Cryst Liq Cryst*, 323: 199-209.
- Varga S, Galindo A and Jackson G (2002b) "Global Fluid Phase Behavior in Binary Mixtures of Rodlike and Platelike Molecules", *J Chem Phys*, 117(15): 7207.
- Varga S, Galindo A and Jackson G (2002b) "Phase Behavior of Symmetric Rod-Plate Mixtures Revisited: Biaxiality Versus Demixing", *J Chem Phys*, 117(22): 10412.
- Varga S, Galindo A and Jackson G (2002c) "Ordering Transitions, Biaxiality, and Demixing in The Symmetric Binary Mixture of Rod and Plate Molecules Described with the Onsager Theory", *Phys Rev E*, 66: 011707.
- Vasilevskaya AS, Kitaeva EL and Sonin AS (1990) "Optically Biaxial Mesophases in Lyotropic Nematics", *Russ J Phys Chem*, 64 (4), 599-601.
- Velego SB, Fleming BD, Biggs S, Wanless EJ and Tilton RD (2000) "Counterion Effect on Hexadecyltrimethylammonium Surfactant Adsorption and Self-Assembly on Silica", *Langmuir*. 16: 2548-2556.
- Wahlstrom EE (1969), *Optical Crystallography*, Fourth Edition, Wiley, London.
- Wensink HH, Vroege GJ and Lekkerkerker HNW (2001) "Isotropic-Nematic Phase Separation in Asymmetrical Rod-Plate Mixtures", *J Chem Phys*, 115(15): 7319.
- Wensink HH, Vroege GJ and Lekkerkerker HNW (2002) "Biaxial Versus Uniaxial Nematic Stability in Asymmetric Rod-Plate Mixtures", *Phys Rev E*, 66: 041704.
- Yu LJ and Saupe A (1980a) "Liquid Crystalline Phases of the Sodium Decylsulfate/Decanol/Water System. Nematic-Nematic and Cholesteric-Cholesteric Phase Transitions", *J Am Chem Soc*, 102: 4879-4883.
- Yu LJ and Saupe A (1980b) "Observation of a Biaxial Nematic Phase in Potassium Laurate-1-Decanol-Water Mixtures", *Phys Rev Lett*, 45: 1000-1003.
- Zana R (1980) "Ionization of Cationic Micelles: Effect of the Detergent Structure", *J Colloid and Interface Sci*, 78: 330-337.

7. CURRICULUM VITAE

Name SURNAME : Emre GÜNER

Place and Date of Birth : İSTANBUL- 07.03.1991

Universities

- Bachelor's Degree : Abant İzzet Baysal University

e-mail : emre_guner_hotmail.com

Address : Bolu Abant İzzet Baysal University, Science
& Art

Faculty, Gököy Campus Bolu

List of Publications :

Akpınar E, Güner E, Ordu O, Neto AMF (2018) “Effect of head group growth of some tetradecylalkylammonium bromide surfactants on obtaining lyotropic biaxial nematic phases” submitted by The European Physical Journal E in 02.11.2018

List of Presentations :

Akpınar E, Güner E, Otluoğlu K and Neto AMF (2016) “Effect of Hofmeister anions on micellization and lyotropic liquid crystalline properties of TDTMABr surfactant molecule”, 28th National Chemistry Congress, 15-21 August, Mersin, Turkey.

Akpınar E, Güner E, Şahin E (2018) “Lyotropic Liquid Crystal Structure of Some Tetradecylalkylammonium Bromide Surfactants”, 1st International Balkan Chemistry Congress, 17-20 September, Edirne, Turkey.

Akpinar E, Guner E and Cetinkaya S (2019) “Micellization Properties of Some Tetradecylalkylammonium bromide Surfactants”, 5th International Conference on New Trends in Chemistry, 22-24 April, Athens, Greece.

